Transportation Research Part D 156 (2026) 105364

Contents lists available at ScienceDirect

Transportation Research Part D

journal homepage: www.elsevier.com/locate/trd

Physics-guided machine learning for ship biofouling assessment in support of maritime decarbonization☆

Xiao Lang [a], Mingyang Zhang [b], Wengang Mao [a,*], Jonas W. Ringsberg [a], Nikolaos Tsoulakos [c]

[a] Department of Mechanical Engineering, Chalmers University of Technology, Gothenburg, Sweden
[b] Department of Mechanical Engineering, Aalto University, Espoo, Finland
[c] Laskaridis Shipping Company, Athens, Greece

ARTICLE INFO

Keywords:
Biofouling
Concept drift
Ship performance
Physics-guided
Decarbonization

ABSTRACT

Ship biofouling significantly increases hull resistance and propeller loading, resulting in increased fuel usage and greenhouse gas emissions. This study presents a physics-guided machine learning approach for detecting performance degradation caused by biofouling. Physics-informed neural networks are first used to generate warm-up data that represent ideal, unfouled ship states under calm water conditions. A baseline model is built from this data and subsequently refined through an incremental learning scheme with new data collected in sliding temporal windows. The resulting incremental models are applied under reference conditions to quantify biofouling-induced performance changes, expressed as key performance indicators. Validation against conventional retraining approaches and the ISO 19030 standard shows that the proposed method more accurately captures both gradual degradation and rapid post-cleaning recovery. By delivering reliable and timely assessments of fouling impact, the framework supports optimized hull and propeller maintenance planning and contributes to improved energy efficiency and emission reduction.

1. Introduction

Shipping accounts for 2.9% of worldwide greenhouse gas (GHG) emissions, releasing around 940 million tons of CO_2 annually. Without intervention, the sector's emission proportion will likely keep increasing (UNCTAD, 2023; IMO, 2020). To address this, the International Maritime Organization (IMO) has introduced more stringent regulatory strategy aimed at reducing emission levels from the shipping industry, prompting ship operators to place greater emphasis on energy efficiency measures to ensure compliance (IMO, 2022). Hull and propeller cleanings of biofouling have been identified as one of the most important and prioritized EEMs for optimizing ship energy efficiency (IMO, 2023a; 2023b). Accurate and reliable biofouling assessment is crucial for optimizing the scheduling of cleaning events, ensuring that cleaning is neither performed earlier, leading to unnecessary maintenance, nor delayed excessively, resulting in increased fuel consumption.

Marine biofouling, which refers to the undesirable accumulation of organisms (such as barnacles, slime, and seaweed grow) on submerged surfaces, is recognized by the IMO as one of the major challenges affecting both the economy and the environment (IMO,

☆ This article is part of a special issue entitled: 'AI-Maritime' published in Transportation Research Part D.

* Corresponding author at: Department of Mechanics and Maritime Sciences, Chalmers University of Technology, Gothenburg, Sweden.
E-mail address: wengang.mao@chalmers.se (W. Mao).

https://doi.org/10.1016/j.trd.2026.105364
Received 1 December 2025; Received in revised form 19 January 2026; Accepted 1 April 2026

2023b). It threatens the balance of marine ecosystems by facilitating the spread of invasive aquatic species and increasing hull roughness, which in turn leads to higher frictional resistance and fuel consumption (Townsin, 2003; Adland et al., 2018). A number of studies have reported on the adverse impact of biofouling on ship performance. Schultz (2007) found that heavy calcareous fouling would lead to an 86% increase in the shaft power required for a navy vessel at cruising speed. Munk et al. (2009) stated that fuel consumption increases by at least 10% on average for lightly fouled hulls, and by up to 35% for heavily fouled hulls. Gundermann and Dirksen (2016) conducted an extensive review of dry-docking maintenance records, examining data from 237 dry-docking events across 210 vessels. Their findings revealed that biofouling could add between 10% and 40% to the resistance of a vessel. Monty et al. (2016) estimated that even sparse tube worm fouling could increase the total resistance of a Very Large Crude Carrier (VLCC) by up to 34%. Owen et al. (2018) evaluated the open water efficiency of the case study propeller, reporting a reduction of up to 30% at the highest simulated fouling level. Uzun et al. (2019) demonstrated that the frictional resistance of a 176-meter-long tanker increased by approximately 32% after one year of operation. A Swedish company evaluated 249 ships and discovered that 44% of them had calcareous fouling covering at least 10% of their hull surfaces, directly linked to up to a 36% increase in propulsion power requirements (I-Tech, 2020).

To mitigate the detrimental effects of biofouling on hulls and propellers, both the IMO and shipping companies have implemented strategies such as applying anti-fouling coatings and scheduling regular hull cleaning (Lam and Lai, 2015). Anti-fouling coatings play an important role in preventing the accumulation of marine organisms, but their cost can be expensive, and some types, such as biocidal self-polishing coatings, may have adverse environmental impacts (Caric et al., 2016). Periodic hull cleaning is the primary measure under the direct control of ship owners. While the rate of fouling is largely influenced by external environmental factors, the frequency and quality of maintenance activities, including hull cleaning and propeller polishing, are decided by the ship owner (Valchev et al., 2022). Aside from dry-docking, hull cleaning is frequently needed to be carried out, such practices do not necessarily ensure that cleaning schedules are optimized (Kjaer et al., 2018). Therefore, to plan these activities reliably and cost-effectively, it is essential to consider the performance losses caused by fouling, aiming to balance between operational efficiency and cost (Schultz et al., 2011). This necessity highlights the importance of establishing transparent and reliable standards for assessing the performance of hulls and propellers.

The purpose of this study is to propose a novel physics-guided incremental machine learning framework to assess the impact of biofouling on ship performance, based on full-scale measurements from two case study chemical tankers. The remainder of this paper is organized as follows. Section 2 reviews related research on assessing the impact of biofouling on ship hull and propeller performance. Section 3 introduces the proposed method for biofouling impact assessment, along with the state-of-the-art method used for comparative analysis. Section 4 details the case study vessels and full-scale measurements, including the associated data processing procedures. Section 5 presents a comparative evaluation of the proposed method against conventional approaches, demonstrating its effectiveness. Finally, Section 6 concludes the paper and outlines directions for future work.

2. Literature review

Ship hull resistance and propeller efficiency cannot be measured directly. The biofouling-induced changes in hull and propeller conditions alter the propulsion power required for maintaining a specified speed through water, even under consistent environmental conditions and operational settings. Thus, to effectively assess biofouling impacts, it is essential to continuously monitor the relationship between propulsion power and ship speed through water across various environmental and operational scenarios.

2.1. Physics-driven methods

Currently, the most widely adopted physical method for assessing the impact of biofouling on hull and propeller performance is the ISO 19030 standard (ISO 19030–1 (ISO, 2016a); ISO 19030–2 (ISO, 2016b); ISO 19030–3 (ISO, 2016c)). This standard outlines methodologies for quantifying changes in hull and propeller performance and defines a suite of maintenance-related performance indicators. It recommends comparing measured performance data against an ideal speed-power reference curve and continuously monitoring this relationship to reliably estimate performance changes. Although the approach is both straightforward and effective, it does exhibit certain limitations and is still under improvement. For example, ISO 19030 requires strict data filtering procedures, but its environmental filtering only considers wind, which may include high wave conditions (Koboevic et al., 2019; Mittendorf et al., 2024). Additionally, the current standard only corrects for wind resistance and does not account for the extra resistance caused by waves, which can significantly affect ship performance (Lang and Mao, 2020).

Various physical approaches have been developed to monitor ship performance changes caused by biofouling. For instance, Logan (2011) employed an empirical formula-based approach to evaluate the propeller performance of two sisterships, using this metric as an efficiency indicator to monitor ship performance degradation resulting from hull fouling. Bialystocki and Konovessis (2016) applied a correction method based on the Beaufort scale to derive fuel consumption and speed curves, parameterized by factors such as ship draft and hull/propeller roughness. Foteinos et al. (2017) utilized noon reports to assess the fouling impact on four Panamax bulk carriers, calculating various resistance components using empirical formulas. Additional studies that employ empirical formulas to quantify the influence of environmental factors on ship performance and by extension, assess biofouling impact can be found in Carchen et al. (2019), Carchen and Atlar (2020), and Valchev et al. (2022). However, due to the assumptions and simplifications inherent in physical modeling, the empirical method may exhibit varying levels of uncertainty when applied to individual ships (Lang et al., 2022).

Physics-based approaches also include computational fluid dynamics (CFD) methods, which have been extensively utilized to quantify the impact of biofouling. For instance, Owen et al. (2018) employed CFD to investigate the effects of various fouling

conditions on propeller performance across different advance coefficients. Song et al. (2019, 2020) integrated CFD with biofouling state specific roughness functions to assess the fouling impact on the hull performance of KCS and KVLCC2 vessels. García et al. (2020) utilized a validated RAN solver, along with experimental investigations of surface roughness properties, to study the effects of fouling on both total ship resistance and frictional resistance. Furthermore, Farkas et al. (2020) applied Granville's similarity law scaling in combination with CFD to examine the influence of fouling on ship resistance and propulsion characteristics. The open-water performance of propellers has also been analyzed using CFD to further evaluate fouling impacts (Farkas et al., 2021). However, CFD methods are computationally expensive and often struggle to accurately model the complex ocean environments encountered by ships, resulting in insufficient accuracy under realistic conditions (Karagiannidis and Themelis, 2021; Lang et al., 2024).

2.2. Data-driven methods

In recent years, data-driven methods have gained increasing popularity in ship performance modeling (Capezza et al, 2019; Uyanık et al, 2020; Yan et al., 2021; Zhang et al., 2024; Fan et al., 2025; Li and Lam, 2025). Yang et al. (2026) proposed a novel attitude-aware spatiotemporal deep learning approach that, for the first time, combined sequential ocean surface images with synchronized IMU-derived motion data through multi-head self-attention, enabling joint modeling of wave dynamics and vessel-induced disturbances. In contrast to physics-based approaches, which require detailed prior knowledge of the underlying physical principles, data-driven techniques rely primarily on data to capture performance characteristics. In the field of biofouling, Coraddu et al. (2019a) employed unsupervised machine learning (ML) techniques based on support vector machines (SVM) and global k-nearest neighbors (KNN), to analyze data from two independent controlled sea trials conducted six months apart, focusing on the effects of biofouling on the hull and propeller. Coraddu et al. (2019b) proposed an extreme learning machine (ELM) method to estimate speed loss caused by marine fouling, demonstrating that their approach provides more accurate and consistent predictions than the ISO 19030 standard for two Handymax chemical/product tankers. Erol et al. (2020) applied detrended fluctuation analysis (DFA) to evaluate the impact of fouling on ship energy performance degradation through continuous monitoring. Laurie et al. (2021) evaluated various ML regression models to predict ship shaft power and used these predictions to generate simulated power-speed curves for assessing performance deterioration caused by biofouling. Shaw and Lin (2021) analyze container ships energy efficiency using the ISO 19030 standard and calculate performance indicators as a reference for monitoring performance and predicting maintenance needs related to biofouling. Gupta et al. (2022) applied nonlinear regression models and probabilistic neural networks to monitor ship performance using in-service data from two sister ships, and predicted performance deterioration caused by fouling.

Traditional machine learning approaches are often based on the assumption that the data distribution remains constant from training to application, treating the data stream as static. However, this simplification ignores the temporal evolution of real-world systems, where input–output relationships may shift due to gradual process variations. In ship performance monitoring, biofouling degrades hull and propeller performance, inducing such drift and causing temporal variations in the speed-power relationship, even when factors like ship draft and weather conditions remain constant. Consequently, these performance variations are not easily captured by conventional ML methods (Zenisek et al., 2019). To address this issue, Mittendorf et al. (2023) employed neural networks with freezing techniques on synthetic datasets to detect concept drift caused by hull biofouling's impact on ship performance. Their machine learning framework was later applied to a cruise vessel operating in the Caribbean Sea to assess performance degradation due to marine growth and benchmarked against the industry standard ISO 19030 (Mittendorf et al., 2024). However, their approach accounts only for wind conditions as prescribed by ISO standards and neglects the influence of encountered waves, which represent the most critical factor affecting ship performance. According to IMO (2012), under representative sea conditions, the ship speed reduction at 75% maximum continuous rating (MCR) can range from approximately 5% to 20%, depending on ship type and loading condition. If not explicitly accounted for, the wave-induced speed reductions could be mistakenly interpreted as biofouling-induced performance degradation.

2.3. Contributions of this study

To sum up, most existing methods exhibit notable research gaps. The ISO 19030 standard neglects the impact of waves on ship performance, thereby conflating wave impact with biofouling effects. Empirical approaches introduce uncertainties due to physical simplifications, while CFD methods are computationally expensive and struggle to represent a large amount of oceanic randomness. Traditional ML techniques fail to address concept drift, and even some state-of-the-art ML studies neglect the critical influence of encountered waves.

To bridge the gaps, we propose a novel physics-guided incremental learning framework to quantify the degree of concept drift as a proxy for the biofouling impact of ship performance. Key contributions are as follows:

- Develop a baseline model established using warm-up data generated by PINNs trained on ship model test results from the case study vessels, to characterize ship performance under ideal conditions, free of wave and biofouling impacts. This model enables accurate estimation of speed reduction during actual operations, and constructing reference baseline.
- Propose an incremental learning strategy by using freezing technology, to detect concept drift. By considering wave conditions and ship operational parameters as input features, the method can effectively detect concept drift caused by biofouling while excluding wave-induced effects.
- Establish a performance assessment metric based on generated reference conditions to quantify the degree of biofouling-induced concept drift.

The proposed framework is demonstrated using long-term full-scale data from two global operation chemical tankers, showing its effectiveness in tracking ship performance degradation caused by biofouling. By enabling data-driven decisions on hull and propeller maintenance, this method supports improved ship energy efficiency and contributes to maritime decarbonization.

3. Problem statement and ISO standard

3.1. Problem statement

The review in Section 2 indicates that most advanced data-driven techniques used to evaluate biofouling effects on ship performance typically rely on static ML models (e.g., SVM, KNN, ELM, DFA). These traditional techniques assume a static relationship between the prediction target and input features across the training and application phases, neglecting the phenomenon of the drift in underlying data concepts that naturally arises within sequential or streaming time series datasets. Formally, concept drift describes time-dependent shifts in the conditional distribution of propulsion power P_D given the input $\boldsymbol{Z}$ (e.g., speed through water, environmental, and operational conditions). Traditional ML models are unable to automatically detect such shifts, instead continuing predictions based on historical training data, thereby potentially losing accuracy over time.

When analyzing biofouling-induced variations, concept drift typically appears as either a gradual or a sudden change. The gradual type indicates incremental performance degradation resulting from the slow accumulation of biofouling, whereas sudden drift is associated with abrupt changes arising from hull and/or propeller cleaning events, including dry docking. Fig. 1 illustrates these two types of concept drift, clearly depicting the temporal impact of biofouling and cleaning events on ship hull and propeller performance. It should be noted that variations in fuel quality and mechanical system degradation are not considered in this study.

3.2. ISO 19030 procedure

The application of the ISO 19030 standard is to establish practical methodologies for quantifying changes in a ship's hull and propeller performance, as well as to define a comprehensive set of performance indicators to guide effective maintenance. The primary parameters are ship speed through water V_w and delivered propulsion power P_D. The assessment procedure of the ISO 19030 standard can be summarized as four steps: (1) data filtering for reference conditions, (2) correction for environmental factors, (3) calculation of performance values (PVs), and (4) calculation of performance indicators (PIs).

Step (1) involves excluding outliers and spike values, while filtering the data for a set of comparable conditions of environmental and operational factors. The filtering follows the default method introduced in the ISO 19030 standard. Outliers are identified using Chauvenet's criterion applied to all measurements in the analysis, defined as:

$$\mathrm{erfc}\left(\frac{\Delta_i}{\sigma \bullet \sqrt{2}}\right) \bullet N < 0.5, \tag{1}$$

where erfc is the complementary error function, N is the number of data points in the considered block, Δ_i is the absolute difference between the i-th measurement (d_i) and the block's mean (μ), and σ represents the standard error of the values in that block. For the

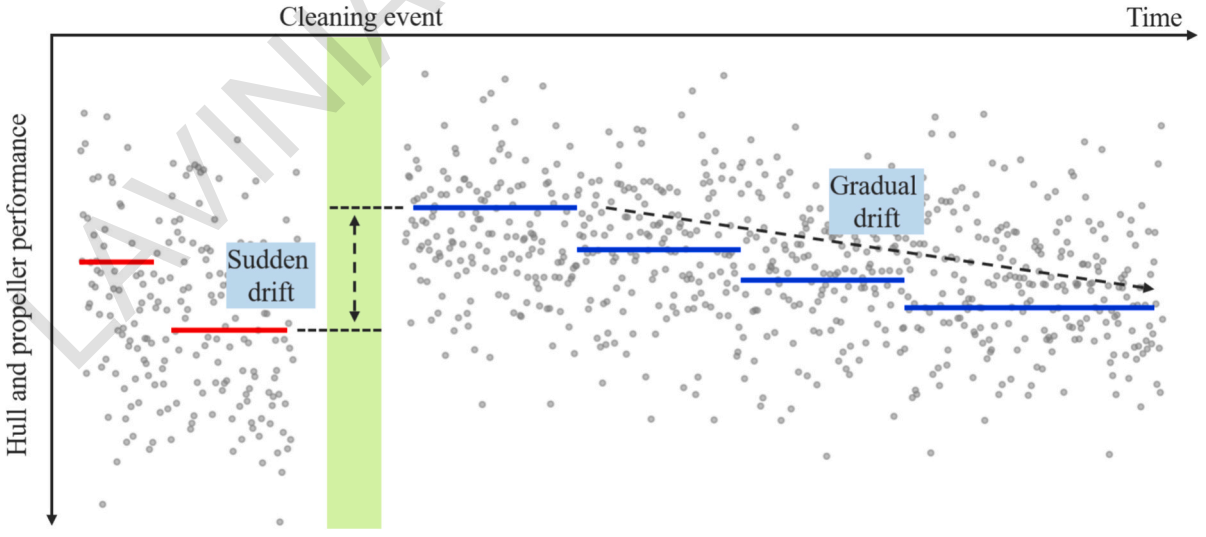

Fig. 1. Illustration of gradual and sudden concept drift in ship hull and propeller performance due to biofouling. Gradual drift represents the incremental deterioration of performance caused by the progressive accumulation of biofouling over time, whereas sudden drift corresponds to abrupt improvements resulting from hull and/or propeller cleaning events.

filtering process, the standard first excludes all data with water temperatures below $+2^{\circ}$C to ensure that the ship is not operating in ice conditions. Next, to eliminate shallow water effects, the water depth (H) must satisfy the following condition:

$$H > \max\left(3\sqrt{B \bullet T},\ 2.75\frac{{V_w}^2}{g}\right), \tag{2}$$

where B is the ship's breadth, T is the mean draft, and g is the gravitational acceleration. The most critical filter is applied to wind conditions: only data with a true wind speed between 0 m/s and 7.9 m/s are retained as reference conditions, thereby excluding metocean conditions associated with a Beaufort number (BN) of 4 or higher. In step (2), the propulsion power P_D is corrected for wind resistance by $P_{D,\mathrm{corr}} = P_D - \Delta P_{\mathrm{wind}}$, where the wind resistance correction ΔP_{wind} is defined as:

$$\Delta P_{\mathrm{wind}} = \frac{(R_{rw} - R_{0w})V_g}{\eta_{D0}} + P_D\left(1 - \frac{\eta_{DM}}{\eta_{D0}}\right), \tag{3}$$

where R_{rw} denotes the wind resistance due to relative wind, R_{0w} represents the air resistance in no-wind conditions, and V_g is the ship speed over ground. Additionally, η_{D0} and η_{DM} correspond to the propulsion efficiency under calm conditions and during the actual voyage. Further details on the wind resistance calculations can be found in ISO 19030–2 (2016). However, the current version of the standard does not include corrections for wave induced added resistance. In step (3), the default PV, ΔV, is calculated as the relative percentage difference between the measured ship speed through water (V_w) and the expected ship speed through water (V_e), as follows:

$$\Delta V = 100 \bullet \frac{(V_w - V_e)}{V_e}. \tag{4}$$

The expected speed, V_e, is determined from a speed-power reference curve corresponding to the $P_{D,\mathrm{corr}}$, and the measured draft. This reference curve can be established through full-scale sea trials, model-scale towing tank tests, or CFD simulations. The speed loss ΔV is subsequently employed as a key performance metric for calculating various PI in step (4). The standard recommends using the average speed loss over a specified period to mitigate uncertainties and smooth out statistically insignificant fluctuations.

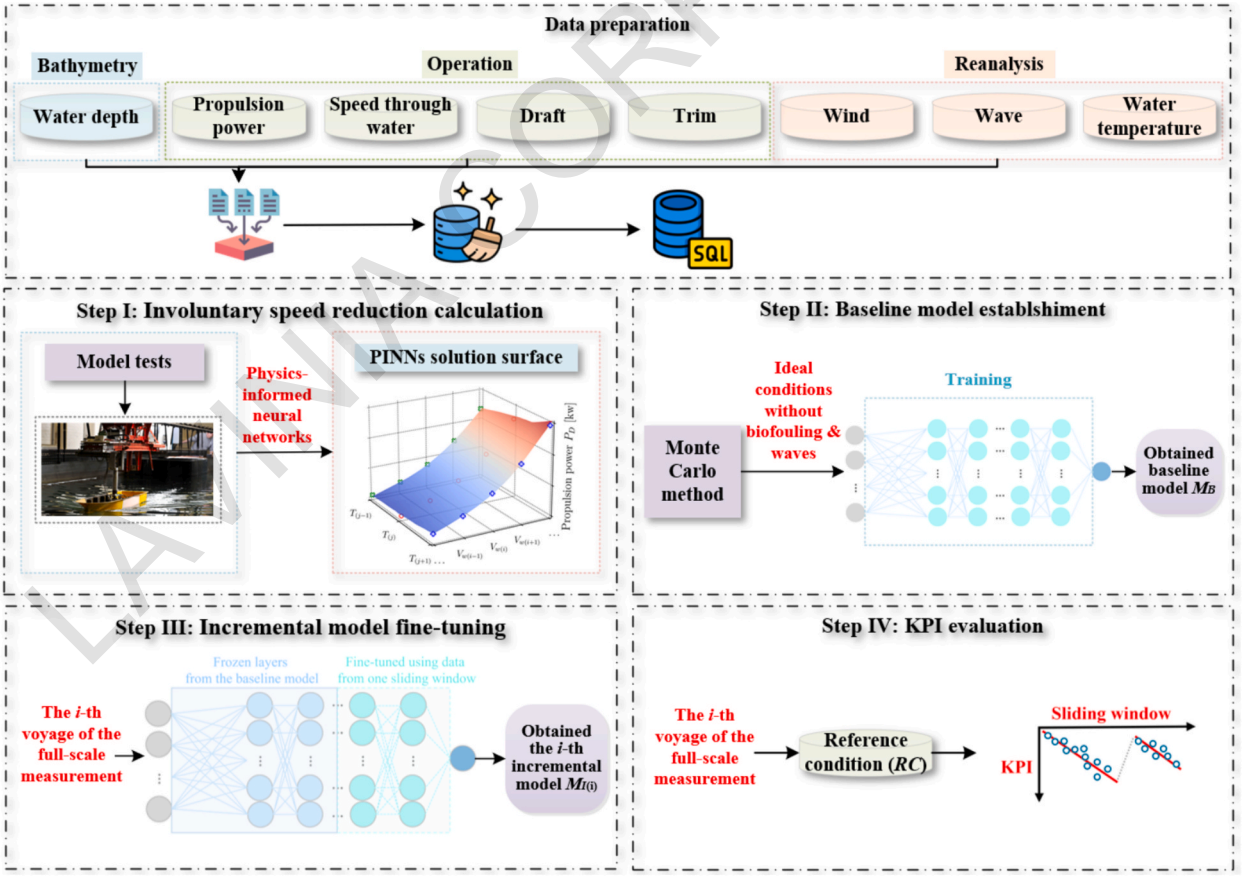

Fig. 2. The proposed method for biofouling impact assessment using incremental machine learning techniques.

4. Methodology

4.1. Modeling architecture

This subsection presents the proposed modeling architecture, which employs incremental learning to detect both gradual and sudden changes in ship performance monitoring data to quantify the impact of biofouling. The overall workflow is presented in Fig. 2.

The data preparation process involves integrating multiple data sources to construct a comprehensive dataset for analysis. The measured parameters include propulsion power (P_D), speed through water (V_w), ship draft (T), and ship trim (T_R). Additionally, using timestamps and location (longitude and latitude) from full-scale measurements, water depth is retrieved from publicly available bathymetry datasets, while wave conditions, wind conditions, and water temperature are obtained from reanalysis data sources. Next, data filtering is performed following the ISO 19030 methodology. Specifically, noise and spike values are removed using Equation (1), shallow-water navigation data is filtered out using Equation (2) to eliminate shallow-water effects, and all records with water temperatures below + 2 °C are excluded to ensure consistency in environmental conditions.

After data preparation, the proposed methodology consists of four main steps:

- Step I: **Involuntary s**peed reduction calculation: In the first step, the propulsion power-speed-draft relationship of the ship under ideal calm water conditions without biofouling is modeled using PINNs (Raissi et al., 2019), trained on ship model test data. Based on this ideal performance model, the involuntary speed reduction ΔV_{abs} caused by biofouling and wave conditions during actual voyages can then be calculated.
- Step II: Baseline model establishment: The baseline model M_B, representing ship performance under ideal conditions, is established using a warm-up dataset generated through Monte Carlo method based on the PINNs developed in Step I. The baseline model provides a benchmark to measure later deviations in involuntary speed reduction within full-scale data streams. The warm-up dataset plays a vital role in characterizing ship performance in the absence of biofouling and wave influence, providing a reliable foundation before adapting to evolving operational conditions.
- Step III: Incremental model refinement: At this step, the baseline model M_B is progressively updated by integrating newly acquired data, each corresponding to a distinct, non-overlapping temporal window (e.g., an individual voyage from port to port). The foundational layers of the original network remain fixed, while the upper layers are updated with new data stream. This progressive adaptation produces a collection of incremental models (M_I) aligned with successive operational windows, ensuring responsiveness to biofouling effects without catastrophic forgetting of baseline information.
- Step IV: KPI evaluation: In the final step, the significant wave height for each voyage is artificially set to zero to establish a reference condition (*RC*) representing hypothetical calm water, free from wave loads. The incremental model developed for that voyage is then applied to the *RC* of that voyage to estimate the speed reduction ΔV_{abs}. The predicted ΔV_{abs} is compared with the expected speed through water V_e under this *RC* to calculate ΔV using Equation (4). This ΔV serves as the KPI for assessing performance degradation specifically attributed to biofouling.

The subsequent subsections present a detailed explanation of each step in the proposed framework.

4.2. Step I: Involuntary speed reduction calculation

To estimate ship performance under ideal conditions, PINNs are developed based on ship model test data. These tests typically provide two-dimensional speed-power measurements across varying draft conditions, as shown in Fig. 3. PINNs extend this by transitioning from two-dimensional observations to a three-dimensional representation, where the measured data points form a continuous surface in the $P_D - V_w - T$ space.

This surface represents a physically consistent solution that models the propulsion power as a function of speed through water and draft. Compared to conventional methods such as bilinear interpolation or polynomial regression, this approach achieves higher accuracy and generalization (Lang et al., 2024). The performance surface is assumed to satisfy a generalized partial differential equation (PDE) of the form:

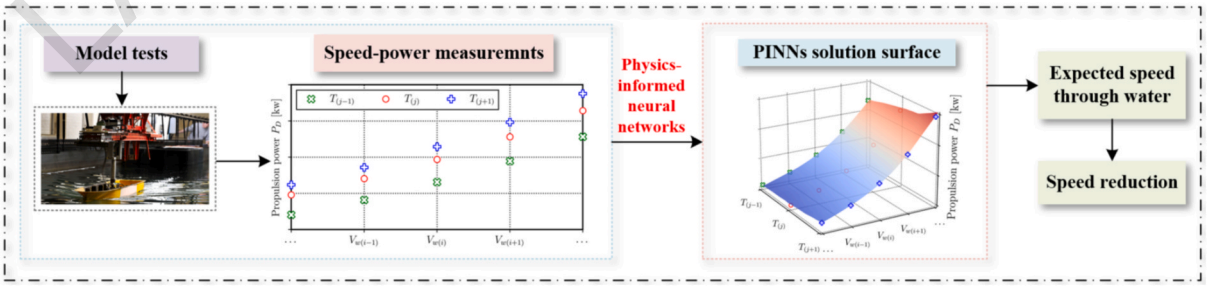

Fig. 3. Detailed modeling of the propulsion power-speed-draft relationship using PINNs to obtain the speed reduction in Step I.

$$a_1\frac{\partial P_D}{\partial V_w}+a_2\frac{\partial P_D}{\partial T}+\mu[P_D,V_w,T;\lambda]=0, V_w\in[V_{wmin},V_{wmax}], T\in[T_{min},T_{max}], \tag{5}$$

where $\mu[P_D,V_w,T;\lambda]$ is the non-linear function capturing complex dependencies, a_1, a_2, and λ are unknow parameters of the PDE. According to the "Cubic Rule", the propulsion power of a ship is commonly assumed to scale with the cube of the speed through water (IMO, 2014). Based on towing tank speed-power measurements, the relationship among propulsion power P_D, speed V_w, and draft T is approximated using the following polynomial expression:

$$P_D=B_1{V_w}^3+B_2{V_w}^2+B_3V_w+B_4V_wT+B_5T^2+B_6T, \tag{6}$$

where B_1 B_6 denote the regression coefficients. The above PDE in Equation (5) contains unknown parameters, i.e., a_1, a_2, and λ, which can be obtained by applying the partial differential operation on Equation (6) with respect to V_w and T, respectively:

$$\frac{\partial P_D}{\partial V_w}=3B_1{V_w}^2+2B_2V_w+B_3+B_4T, \tag{7}$$

$$\frac{\partial P_D}{\partial T}=B_4V_w+2B_5T+B_6. \tag{8}$$

By rearranging Equations (7) and (8), a PDE describing the relationship between propulsion power, speed, and draft can be obtained:

$$\frac{2B_5}{B_4}\frac{\partial P_D}{\partial V_w}-\frac{\partial P_D}{\partial T}-\frac{6B_1B_5}{B_4}{V_w}^2-\left(\frac{4B_2B_5}{B_4}-B_4\right)V_w-\left(\frac{2B_5}{B_4}B_3-B_6\right)=0. \tag{9}$$

Comparing Equation (9) with the generalized PDE form in Equation (5), there exist the following relationship:

$$a_1=\frac{2B_5}{B_4},\ a_2=-1,\ \mu[P_D,V_w,T;\lambda]=-\left(\frac{6B_1B_5}{B_4}{V_w}^2+\left(\frac{4B_2B_5}{B_4}-B_4\right)V_w+\left(\frac{2B_5}{B_4}B_3-B_6\right)\right). \tag{10}$$

A neural network $h(V_w,T)$ is then introduced to approximate the propulsion power P_D. Thus Equation (5) is reformed as:

$$g:=a_1\frac{\partial h}{\partial V_w}+a_2\frac{\partial h}{\partial T}+\mu[h,V_w,T;\lambda],V_w\in[V_{wmin},V_{wmax}],T\in[T_{min},T_{max}]. \tag{11}$$

To enforce physical consistency, the PINN is trained by minimizing a composite loss function that includes both the residual of the governing equation and the mismatch with measured boundary data:

$$MSE=MSE_{bc}+MSE_g, \tag{12}$$

where MSE_{bc} quantifies the discrepancy between the network $h(V_w,T)$ output and the boundary condition data obtained from towing tank experiments. The approximator network $h(V_w,T)$ contains trainable weights and biases and aims to predict propulsion power given the ship speed through water and draft. While MSE_g represents the residual of the governing PDE, is evaluated through automatic differentiation and serves solely to enforce the physical constraints during training (remains untrained). The trained PINNs thus approximates the P_D-V_w-T relationship under calm water conditions. Further details on parameter determination and implementation can be found in Lang et al. (2024). Hyperparameters, including network layer, neuron numbers, and learning rate, follow the validated settings reported therein and were not further tuned in this study to ensure model stability and reproducibility.

The corrected propulsion power ($P_{D,\,\mathrm{corr}}$) obtained from ISO 19030 standard Equation (3), and the measured draft (T) are used as inputs, allowing the expected speed through water (V_e) under ideal calm water conditions to be reverse calculated using PINNs. Finally, by comparing V_e with the measured ship speed through water V_w, the involuntary speed reduction caused by biofouling and encountered waves is quantified as:

$$\Delta V_{\mathrm{abs}}=V_e-V_w. \tag{13}$$

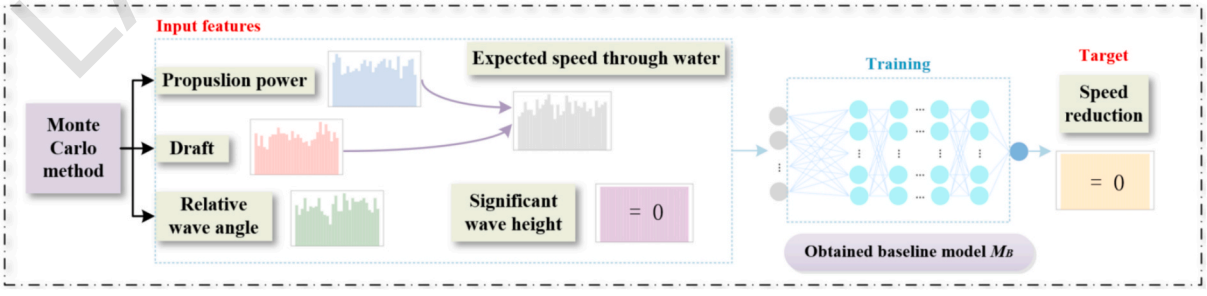

Fig. 4. Structure of the multi-layer neural network adopted in Step II to model speed reduction under baseline conditions.

4.3. Step II: Baseline model establishment

In this study, regression-based ANNs is utilized to establish the baseline performance model (Specht, 1991). Fig. 4 shows that the network includes an input layer, a series of hidden layers, and an output layer, enabling it to capture the nonlinear relationships between ship performance parameters. The input features $\boldsymbol{X}$ for the baseline model include corrected propulsion power $P_{D,\mathrm{corr}}$, ship draft T, ideal ship speed V_e, significant wave height H_s, and relative wave angle β. Since the impact of wind resistance on propulsion power has already been corrected, the most critical external factors affecting the ship's speed-power relationship are wave conditions. The prediction target is speed reduction ΔV_{abs}.

The baseline model M_B is constructed to represent ship performance in the absence of biofouling and wave-induced resistance. This requires a warm-up period dataset for training, which ideally consists of ship performance data under conditions with no waves and no biofouling. In real-world monitoring data, instances with both small waves and no biofouling accumulation are extremely limited. To overcome this limitation, the proposed method generates the warm-up dataset using the PINNs established in Step I. First, a set of propulsion power-draft ($P_{D,\mathrm{corr}}$-T) pairs is generated using the Monte Carlo method. The draft T is sampled between T_{min} corresponding to the ballast loading condition, and T_{max} corresponding to the scantling loading condition. The corrected delivered power $P_{D,\,\mathrm{corr}}$ is sampled within a range, bounded by the minimum power at V_{wmin} under ballast condition, and the maximum power at V_{wmax} under scantling condition. A total of 500 data points is generated within the specified ranges following a uniform sampling strategy, ensuring unbiased and comprehensive coverage of the ideal operating conditions of the ship. The corresponding V_e are then computed using the PINNs model. Since the warm-up data represents ideal calm water conditions without biofouling, all H_s and speed reduction ΔV_{abs} in this dataset are set to zero. The relative wave angle β is randomly generated using the Monte Carlo method within a range of 0 (head sea) to 180 (follow sea) degrees, consistent with the distribution observed in the measured data.

Generally, an ANN can be formulated as a composite function made up of multiple computational layers. For instance, the prediction of speed reduction ΔV_{abs} can be expressed functionally as:

$$\widehat{\Delta V_{\mathrm{abs}}} = F(\Theta, \boldsymbol{X}) = f_l[\Theta_l, f_{l-1}(\Theta_{l-1}, \cdots, f_1\{\Theta_1, \boldsymbol{X}\})]. \tag{14}$$

As presented in Equation (14), the neural network establishes a feedforward relationship in which the input vector $\boldsymbol{X} = \{P_{D,\mathrm{corr}},\ T,\ V_e,\ H_s,\ \beta\}$ propagates hidden layers to the predicted $\widehat{\Delta V_{\mathrm{abs}}}$. Each layer l in the network is characterized by a set of parameters Θ, and an associated activation function f. The Rectified Linear Unit (ReLU) is employed in this work as the activation function owing to its effectiveness in mitigating the vanishing gradient issue.

4.4. Step III: Incremental model fine-tuning

Incremental learning can be viewed as a sequential adaptation process, where the model is repeatedly updated with new batches of data (Parisi et al., 2019). In this study, the method is applied to identify biofouling-related concept drift for the same vessel by analyzing datasets collected across distinct time intervals. Incremental learning algorithms inherently encounter the stability-plasticity dilemma (French, 1999). To address concept drift effectively, the model must achieve a balance between stability and plasticity. This balance allows continual learning systems to incorporate newly arriving information while simultaneously preserving knowledge obtained from earlier training phases. A basic form of incremental learning simply retrains the whole model on the expanded dataset, without employing mechanisms to regulate how previous knowledge is maintained. Although such an approach offers full adaptability to incoming data, it is particularly vulnerable to catastrophic forgetting of earlier representations.

Within the proposed framework, parameter freezing, commonly employed in transfer learning, is utilized to reduce the risk of catastrophic forgetting. Similar strategies have been explored in previous research (Jung et al., 2016; Ramasesh et al., 2020). We denote a domain by $\mathscr{D}$, which is characterized by its feature space and the probability distribution defined over that space. A task $\mathscr{T}$ describes the objective of mapping input variables to their corresponding outputs. In this study, both the source and target domains, along with their respective tasks, are defined as follows:

- $\mathscr{D}_{\mathrm{source}} = \{\boldsymbol{X}_{\mathrm{source}}, p(\boldsymbol{X}_{\mathrm{source}})\}$: represents the operational parameters obtained during the warm-up stage.
- $\mathscr{D}^{(i)}_{\mathrm{target}}$: corresponds to the dataset collected during the i-th voyage, reflecting evolving operational conditions that require the model to perform incremental adaptation.
- $\mathscr{T}_{\mathrm{source}}$: aims to predict the speed reduction using the warm-up dataset, and is defined as:

$$\mathscr{T}_{\mathrm{source}} = \{\Delta \boldsymbol{V}_{\mathbf{abs}\,\mathrm{source}}, F_{\mathrm{source}}(\Theta_{\mathrm{source}}, \boldsymbol{X}_{\mathrm{source}})\}, \tag{15}$$

  where $\Delta \boldsymbol{V}_{\mathbf{abs}\,\mathrm{source}}$ denotes the label space (speed reduction), and $F_{\mathrm{source}}(\Theta_{\mathrm{source}}, \boldsymbol{X}_{\mathrm{source}})$ is the predictive function of the baseline model parameterized by Θ_{source}.

- $\mathscr{T}^{(i)}_{\mathrm{target}}$: defines the i-th voyage-specific adaptation process, in which the baseline model is updated to predict the speed reduction for new observations. It is given by:

$$\mathscr{T}^{(i)}_{\mathrm{target}} = \left\{\Delta \boldsymbol{V}^{(i)}_{\mathbf{abs}\,\mathrm{target}}, F^{(i)}_{\mathrm{target}}\left(\Theta^{(i)}_{\mathrm{target}}, \boldsymbol{X}^{(i)}_{\mathrm{target}}\right)\right\}. \tag{16}$$

Here, $\Delta \boldsymbol{V}_{\mathbf{abs}\,\mathrm{target}}^{(i)}$ and $\boldsymbol{X}_{\mathrm{target}}^{(i)}$ denote the output label (speed reduction) and the corresponding input features for the i-th voyage. The predictive function $F_{\mathrm{target}}^{(i)}$ is refined within each time window through fine-tuning of its parameters $\Theta_{\mathrm{target}}^{(i)}$.

In the context of incremental learning, this process can be viewed as a series of learning episodes, each corresponding to a distinct temporal segment of the collected dataset. Every voyage introduces a new learning instance that necessitates an appropriate update of the model parameters. The problem thus can be represented as follows:

$$\mathscr{T}_{\mathrm{target}} = \left[\mathscr{T}_{\mathrm{target}}^{(1)}, \mathscr{T}_{\mathrm{target}}^{(2)}, \cdots, \mathscr{T}_{\mathrm{target}}^{(n)}\right], \tag{17}$$

where n is the total number of the considered voyages. Each task is defined by a new voyage dataset, with the i-th voyage corresponding target domain evolving as:

$$\mathscr{D}_{\mathrm{target}}^{(i)} = \left\{\boldsymbol{X}_{\mathrm{target}}^{(i)}, p\left(\boldsymbol{X}_{\mathrm{target}}^{(i)}\right)\right\}. \tag{18}$$

To handle concept drift, the model is progressively refined for each target domain, maintaining the information inherited from the baseline model. The corresponding freezing framework is illustrated in Fig. 5.

In this configuration, the deeper layers of the baseline network remain unchanged to preserve the fundamental representations learned in the warm-up stage, whereas the higher layers are updated with newly acquired data from each voyage. This strategy enables the model to adjust to changing operational conditions while preserving previously acquired knowledge.

The incremental fine-tuning process using frozen layers is formulated as an optimization task for each time window, expressed as:

$$\Theta_u^{(i)} = \underset{\Theta_u}{\mathrm{argmin}} L\left\{\Delta \boldsymbol{V}_{\mathbf{abs}\,\mathrm{target}}^{(i)}, F_{\mathrm{target}}^{(i)}\left(\boldsymbol{X}_{\mathrm{target}}^{(i)}; \Theta_f, \Theta_u\right)\right\}, \tag{19}$$

where Θ_f denotes the parameter set of the layers kept fixed to maintain the representations established in the warm-up stage, while Θ_u refers to the parameters of the layers updated during fine-tuning. The loss function L is employed to reduce the prediction error associated with the i-th voyage.

4.5. Step IV: KPI evaluation

In the final step, the proposed methodology evaluates the KPI to quantify the effect of biofouling on ship performance. As illustrated in Fig. 6, for each voyage, the significant wave height is artificially set to zero, establishing the *RC* corresponding to hypothetical calm water without wave loads. The incremental model $M_{I(i)}$, developed for the i-th voyage, is then applied to this *RC* to predict the involuntary speed reduction ΔV_{abs}.

The KPI on the i-th voyage is defined as the relative speed loss $\Delta V_{(i)}$, calculated by comparing the predicted speed reduction under the *RC* with the expected ship speed $V_e(RC)$:

$$\Delta V_{(i)} = 100 \bullet \mu\left[\frac{-M_{I(i)}(RC)}{V_e(RC)}\right]. \tag{20}$$

Finally, the sequence of $\Delta V_{(i)}$ values across voyages is tracked over sliding windows (see Fig. 6). This KPI serves as a standardized metric to monitor gradual and sudden performance degradation, isolating the specific contribution of biofouling while filtering out the influence of waves and wind. This KPI is also consistent with the default ISO 19030 method, which adopts percentage speed loss as the primary performance change indicator.

5. Full-scale measurements and case studies

5.1. Case study vessels and data acquisition

Two sister ships are investigated as case study vessels, referred to as S1 and S2, which belong to the same type of worldwide operating chemical tanker, primarily sailing between Europe, Asia, and the Americas. Full-scale measurement data for both vessels are available from 2014 to 2018. These chemical tankers have the length between perpendiculars of 174.8 m, breadth of 32.2 m,

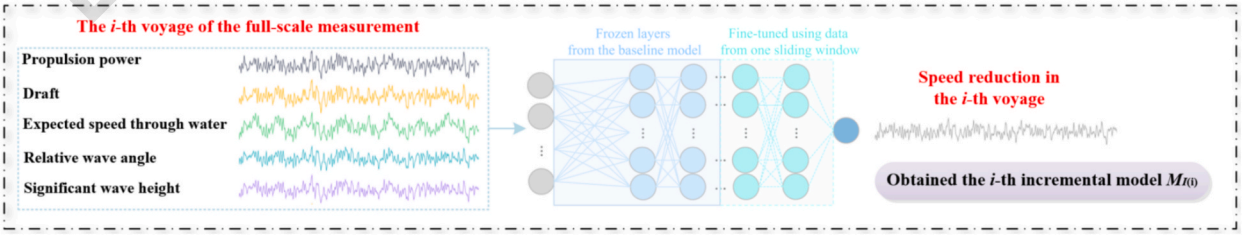

Fig. 5. Illustration of the freezing-based incremental learning framework employed in Step III.

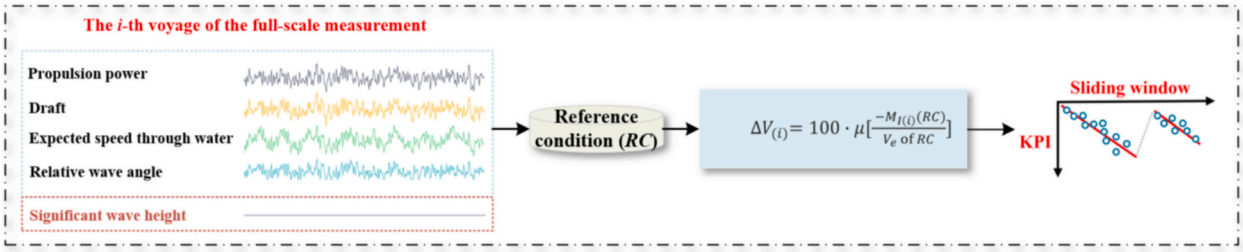

Fig. 6. Schematic representation of Step IV, showing the KPI evaluation process under the *RC*.

deadweight of over 46,000 tons, and design draft is 10.98 m. The speed-power data under calm water conditions is available from towing tank model tests under three loading conditions: $T \in$[6.9 m, 10.98 m, 12.18 m], as shown in Fig. 7(a). Fig. 7(b) presents the solution surface of the PDE established by the PINNs at different drafts. The detailed modeling procedure for the case study chemical tankers can be found in Lang et al. (2024).

The raw measurements were recorded at a frequency of 1 Hz and subsequently down-sampled to 15-minute mean values. The dataset includes propulsion power, speed through water, ship draft, ship trim, ship location, heading, etc. In addition, each data point is labeled according to the vessel's operational status: sea passage, at anchor, at berth, or manoeuvring. Fig. 8 shows the measured propulsion power for ships S1 and S2 from February 2014 to the end of 2018. Different background colors indicate different operational modes, and the cleaning events, as provided by the shipowner, are marked with green lines. Each ship underwent one dry docking during the five-year operation period: S1 in January 2015 and S2 in November 2015, marked with red lines.

For the ISO 19030 standard and proposed incremental learning method, required variables such as water depth H, wave and wind conditions, and sea water temperature are not directly measured by the case study vessels. In this study, global water depth data are obtained from the publicly available ETOPO1 bathymetry dataset provided by the National Oceanic and Atmospheric Administration (NOAA), with a spatial resolution of $0.0167^\circ \times 0.0167^\circ$ (Amante and Eakins, 2009). The encountered metocean parameters, including mean wave direction θ, significant wave height H_s, wind speed U_{wind} and V_{wind} are retrieved from the ERA5 reanalysis dataset, which provides hourly data at a spatial resolution of $0.5^\circ \times 0.5^\circ$ (Copernicus Climate Change Service (C3S), 2019). Water depth H is matched using two-dimensional spatial interpolation based on the ship's recorded latitude and longitude. While wave and wind conditions are obtained using three-dimensional spatiotemporal interpolation, incorporating both spatial coordinates and timestamps. Finally, the relative wave angle β is calculated using the ship's heading and the matched mean wave direction.

5.2. Data preprocessing

Data analysis in this research is exclusively focused on measurements recorded during sailing periods, excluding any data collected during maneuvering. Therefore, the first step in the data processing procedure is to extract the sea passage operational mode data for ships S1 and S2, as shown in Fig. 8. For ship S1, only 51% of the total data were retained, while for S2, the percentage is 45%, indicating that both vessels spent nearly half of the recorded time in anchor or at berth conditions. When down-sampling the high-frequency 1 Hz measurements to 15-minute mean values, Equation (1) is applied to filter outliers and spike values, ensuring data quality and consistency. Subsequently, shallow-water navigation data are filtered out using Equation (2) to eliminate the influence of shallow-water

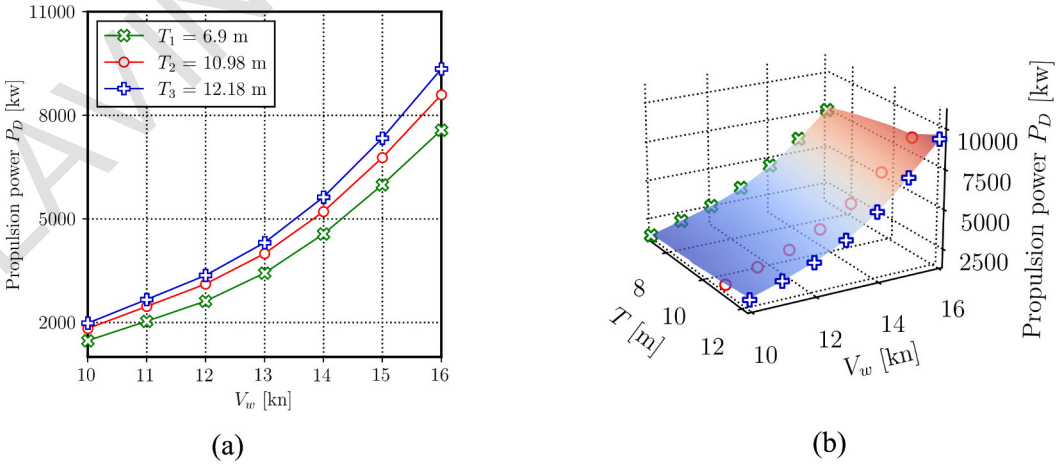

Fig. 7. The case study chemical tankers: (a) speed-power measurements from towing tank model tests, (b) PDE's solution surface at different drafts established by PINNs.

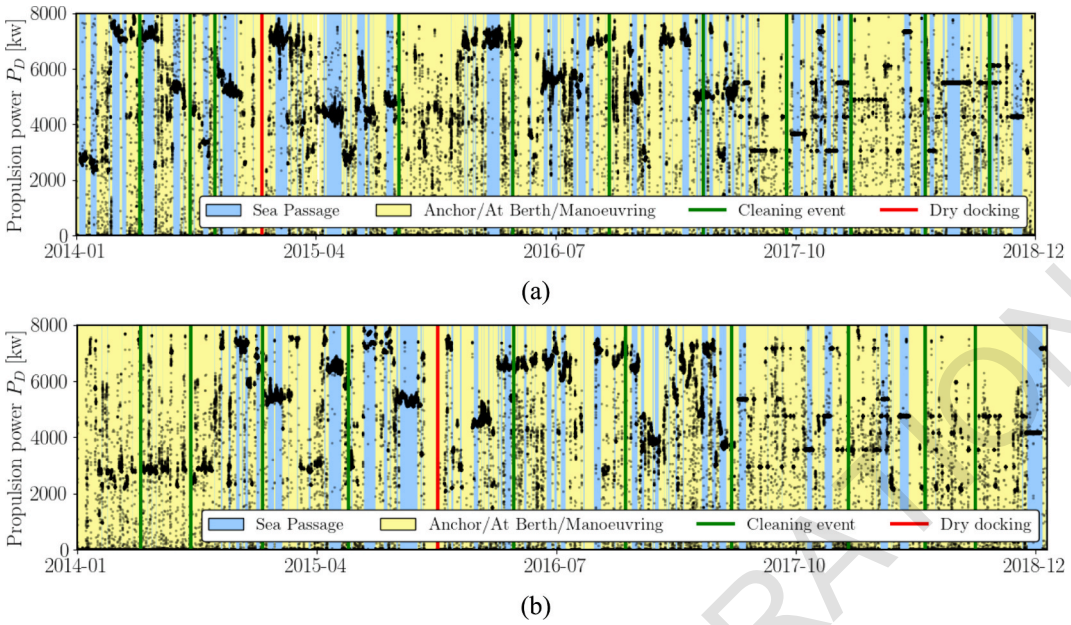

Fig. 8. Measured propulsion power P_D from 2014 to 2018 for (a) ship S1 and (b) ship S2. The background shading distinguishes operational modes (sea passage, anchoring, at berth, or manoeuvring), and green lines indicate recorded cleaning events, and red line indicate dry docking. (For interpretation of the references to colour in this figure legend, the reader is referred to the web version of this article.)

effects. Furthermore, all records with water temperatures below + 2 °C are excluded to ensure that the vessels were not operating in icy conditions.

Among all measured parameters, speed through water V_w is the most critical for assessing the impact of biofouling. However, V_w, measured using a Doppler log is susceptible to various sources of error, including sensor fouling, water turbidity, high wave conditions, and the ship's trim. To improve the reliability of V_w measurements, the method proposed by Ikonomakis et al. (2021) is applied, which filters out data where the absolute difference between speed through water and speed over ground exceeds 2 knots, i.e., $|V_w\text{-}V_g| \leq 2$ knots. Furthermore, to ensure that the speed reduction ΔV_{abs} estimated from the PINNs remains within the valid experimental range, only data falling within the speed and draft ranges of the towing tank model tests are retained: $10 \leq V_w \leq 16$ knots, $6.9 \leq T \leq 12.18$ meters. Finally, the wind components U_{wind} and V_{wind}, obtained from the reanalysis dataset, are combined to calculate the true wind speed as the magnitude of the wind vector. Following the recommendation of ISO 19030, all data points with true wind speed exceeding 7.9 m/s are filtered out. Consequently, the temporal window for incremental model updating corresponds to all data during a voyage's sea passage after data preprocessing.

5.3. Data analysis

After the data preprocessing described above, harsh weather conditions with true wind speeds greater than 7.9 m/s were filtered out in accordance with the ISO 19030 standard, corresponding approximately to BN-4 and above. However, under this filtering condition, the wave height still reaches up to 2 m, which can substantially affect the ship performance. The added resistance due to waves may lead to involuntary speed reductions that could be mistakenly attributed to biofouling. Thus, Figs. 9 and 10 present the distributions of true wind speed and significant wave height in the final preprocessed dataset for ships S1 and S2, respectively.

As shown in Figs. 9 and 10 (right), the true wind speed for ships S1 and S2 is filtered in the range of 0 to 7.9 m/s. However, in terms

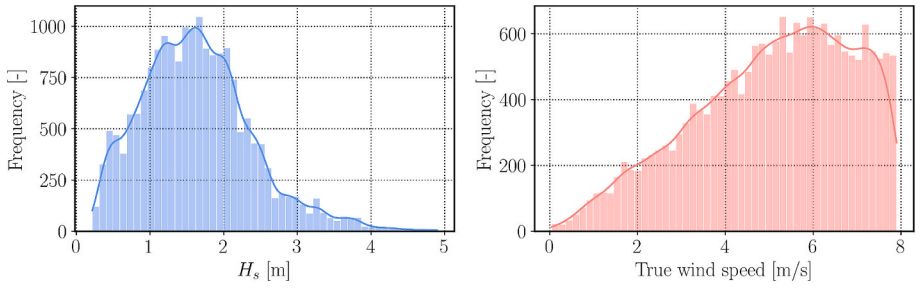

Fig. 9. Distributions of significant wave height H_s (left) and true wind speed (right) in the preprocessed dataset for ship S1.

of significant wave height H_s, ship S1 exhibits a wide distribution of near 2 m, with many data even exceeding 3 m or more, as shown in Fig. 9 (left). A similar distribution is observed for ship S2 in Fig. 10 (left), with a considerable number of wave heights exceeding 2 m and some reaching over 3 m. This indicates that the ISO 19030 filtering method, based solely on true wind speed, fails to fully exclude harsh wave conditions. Moreover, while ISO 19030 includes correction procedures for wind effects, it does not address the impact of waves on ship performance. These harsh sea states can lead to substantial errors and uncertainty in biofouling impact assessments.

Fig. 11 illustrates the scatter of measured ship speed through water V_w and wind-corrected propulsion power $P_{D,\,\mathrm{corr}}$ for ship S1 and S2. The speed range on the x-axis of Fig. 11 spans approximately 10 to 15 knots, with the maximum observed speed difference at the identical power levels being less than 4 knots, corresponding to a speed reduction of roughly 30%. As indicated by the color bar, these large speed reductions are associated with significant wave heights of approximately 3 m and, in some cases, exceeding 4 m. Under such harsh wave conditions, wave-induced speed reduction is substantial. These observations further demonstrate that using such data to derive performance indicators under the ISO 19030 framework could conflate the effects of waves and biofouling. To ensure a more robust analysis, a stricter filtering criterion based on wave height is applied in Section 6 to define a comparison reference. Only data with wave heights below 0.6 m (i.e., BN-2 or calmer conditions) are retained as the comparison reference, following the range definitions recommended in ISO 15016 (ISO, 2015). This additional filtering minimizes the impact of wave-induced loads, providing a more accurate basis for assessing biofouling effects.

6. Results and discussion

In this section, the proposed freezing-based incremental learning method is developed and evaluated using the full-scale measurement data from the two case study sister ships. Its effectiveness is assessed by comparing the results against two benchmarks: the ISO 19030 standard and a traditional incremental learning model employing the retraining approach.

To more accurately quantify biofouling-induced ΔV and minimize uncertainties arising from wave loads that persist even after ISO 19030 filtering, an additional filtering step is applied. Specifically, only data with significant wave heights H_s below 0.6 m are retained, corresponding to BN-2 or calmer conditions. While this stricter filtering reduces the number of available voyages for analysis, it provides a more reliable reference by ensuring minimal impact from wave-induced loads, thereby enhancing the robustness of performance evaluations.

6.1. ISO 19030 standard

The KPI ΔV for each voyage obtained by the ISO 19030 standard method for the case study ship S1 is presented in Fig. 12. Different color frames indicate the intervals between successive cleaning events. The background black scatter points represent the ΔV values calculated using the ISO 19030 default filtering procedure for all sea passage data after preprocessing, which exhibit considerable fluctuations. The variation in color intensity reflects the local data density, where darker regions correspond to a larger number of retained data points, while lighter regions indicate fewer data points due to data filtering. The black cross markers shown in the figure represent the average KPI values for each voyage calculated using the ISO 19030. The maximum ΔV for individual voyages is approximately 13%, while the minimum is around 1%. This high variability suggests substantial uncertainty in the results obtained through the standard filtering approach, as data associated with large significant wave heights are still retained. In contrast, the red cross markers represent the results obtained using the stricter BN-2 filtering, where only data with significant wave heights below 0.6 m are considered. Due to the stringent filtering criterion, only nine voyages contain sufficient low-wave data (at least 10 h of sailing) to be evaluated.

As listed in Table 1, for the nine considered voyages, the ΔV discrepancies between the ISO 19030 standard and the BN-2 filtering method generally range from 1% to 2% under relatively calm sea conditions. However, when the voyages encounter moderate waves, the discrepancies increase significantly, reaching up to approximately 4%.

Specifically, voyage 1 encountered head seas exceeding 2 m, resulting in an additional speed reduction of approximately 5.4%. In the case of voyage 9, which experienced beam seas over 2 m, the wave-induced speed reduction was approximately 2.5%. Similarly, voyage 3 faced nearly 3 m beam seas, leading to a speed reduction of more than 4%. Additionally, as shown in Fig. 12, even with the default ISO 19030 filtering, there are insufficient voyages within each interval between cleaning events to provide a robust basis to detect the biofouling impact trend.

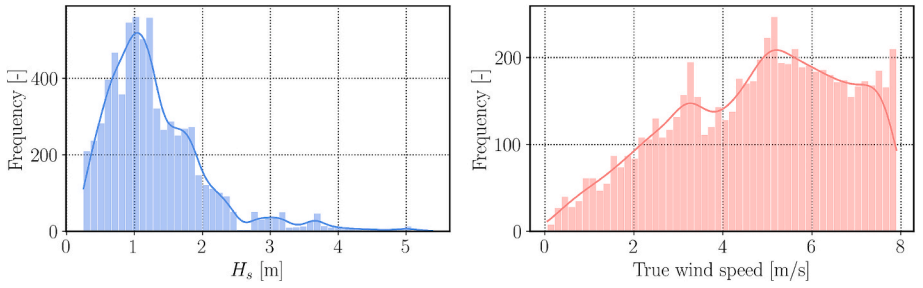

Fig. 10. Distributions of significant wave height H_s (left) and true wind speed (right) in the preprocessed dataset for ship S2.

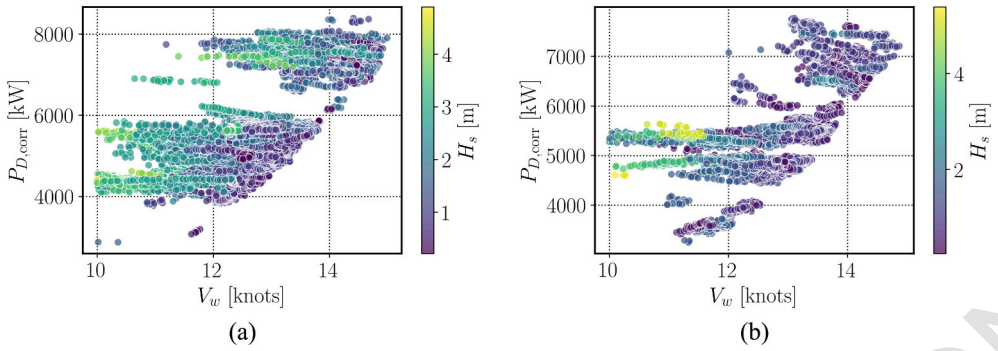

Fig. 11. Scatter plots of corrected propulsion power $P_{D,\mathrm{corr}}$ versus measured speed through water V_w, with color indicating significant wave height H_s, for (a) ship S1 and (b) ship S2.

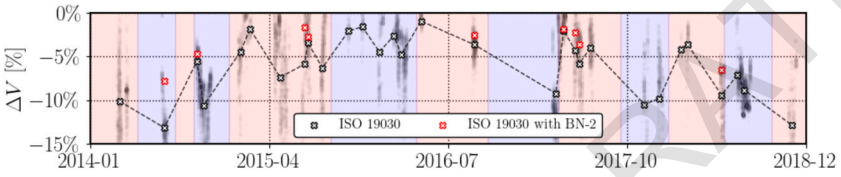

Fig. 12. Comparison of KPI (ΔV) for ship S1 calculated using the ISO 19030 standard (black cross markers) and the stricter BN-2 filtering (red cross markers). Different background colors frames indicate the intervals between cleaning events, and the background black scatter represents ΔV values calculated for all sea passage data after preprocessing. (For interpretation of the references to colour in this figure legend, the reader is referred to the web version of this article.)

Similarly, the results for the case study ship S2 are presented in Fig. 13 and Table 2. Before 2015, most of the voyages for S2 involved short-distance transport, resulting in limited usable data after applying the ISO 19030 default filtering. Within each interval between cleaning events, only a single voyage was typically available. After the dry docking in 2015, longer voyages became more frequent, providing a slightly larger dataset for analysis.

The maximum ΔV for individual voyages reaches approximately 15%, while the minimum is around 2%, as shown in Fig. 13. After applying the BN-2 filtering, only nine voyages remain available for comparison. Similar to the findings for ship S1, the ΔV discrepancies between different filtering methods for ship S2 generally range from 1% to 2% under relatively low wave conditions. However, as wave height increases, the difference in the detected ΔV also becomes more pronounced. For example, voyage 4 and voyage 6, which encountered approximately 2-meter beam seas and bow seas, exhibit discrepancies of around 2% and 3%, respectively. In contrast, voyage 7, which experienced bow seas ranging from 3 to 4 m, shows a significantly higher discrepancy, exceeding 6%.

Overall, the ISO 19030 standard significantly limits the number of usable voyages for analysis due to its default filtering method. Additionally, because the filtering process relies solely on true wind speed and only applies corrections for wind loads, voyages encountering waves exceeding 2 m will have their calculated ΔV influenced by both biofouling and wave impacts. This conflation introduces considerable noise and error into the assessment of the ship's actual biofouling condition, undermining the reliability of the results.

6.2. *Comparison of the proposed method and retrain method under ISO 19030 filtering*

The proposed freezing-based incremental learning model is applied for comparison with the retraining method using data from the

Table 1
KPI (ΔV) values using the ISO 19030 standard and the BN-2 filtering method for nine considered voyages of ship S1.

Voyage ID	ISO 19,030	ISO 19,030 with BN-2
1	13.15%	7.73%
2	5.53%	4.68%
3	5.86%	1.69%
4	3.42%	2.76%
5	3.62%	2.49%
6	2.06%	1.83%
7	4.32%	2.20%
8	5.79%	3.62%
9	9.40%	6.47%

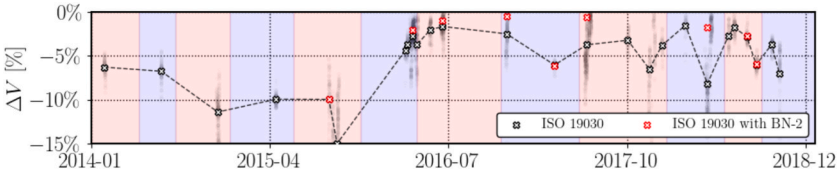

Fig. 13. Comparison of KPI (ΔV) for ship S2 calculated using the ISO 19030 standard (black cross markers) and the stricter BN-2 filtering (red cross markers). Different background colors frames indicate the intervals between cleaning events, and the background black scatter represents ΔV values calculated for all sea passage data after preprocessing. (For interpretation of the references to colour in this figure legend, the reader is referred to the web version of this article.)

Table 2
KPI (ΔV) values using the ISO 19030 standard and the BN-2 filtering method for nine considered voyages of ship S2.

Voyage ID	ISO 19,030	ISO 19,030 with BN-2
1	9.94%	9.93%
2	2.71%	2.05%
3	1.63%	0.98%
4	2.46%	0.43%
5	6.03%	6.09%
6	3.73%	0.58%
7	8.17%	1.78%
8	2.76%	2.71%
9	5.97%	5.90%

two case study ships in this subsection. This comparison is conducted in two steps. First, only data filtered through BN-2 conditions are used to perform incremental fine-tuning for the proposed method and retraining for the retrain method. The purpose of this step is to benchmark the accuracy of each approach against the ΔV values obtained from ISO 19030 with BN-2 filtering, thereby assessing whether the methods can achieve consistent results with measured values under calm sea conditions.

For ship S1, the results for the nine voyages considered are shown in Fig. 14. The ΔV values derived from ISO 19030 with BN-2 filtering are indicated by red markers, while the results from the proposed method are displayed as blue scatters, and those from the retrain method are represented by green scatters. The corresponding percentage differences are summarized in Table 3, which quantifies how closely each learning strategy reproduces the reference KPI derived from ISO 19030 with BN-2. The proposed method demonstrates good consistency with the ISO 19030 with BN-2 reference data as presented in the figure, with most KPI ΔV discrepancies remaining within 0.5%. In contrast, the retrain method exhibits significant inaccuracies. Due to the limited availability of BN-2 data for each voyage, the retrained models tend to retain characteristics of the warm-up data, resulting in consistently low ΔV predictions, with most values below 1%. This indicates an inability to accurately capture the speed changes induced by biofouling.

For ship S2, similar results are obtained, as shown in Fig. 15 and Table 4. The discrepancy of KPI (ΔV) values derived from the proposed method are slightly higher than those obtained for ship S1 when compared against the ISO 19030 with BN-2 filtering. However, the discrepancies remain within approximately 1%, demonstrating the robustness of the proposed method to catch up with the real trend. In contrast, the retrain method continues to retain patterns learned from the warm-up data, resulting in consistently low ΔV values. This indicates its inability to accurately capture the true impact of biofouling on ship performance by using limited BN-2 data.

The second stage of the comparison is based on data obtained using the default filtering of ISO 19030, which provides a larger number of voyages for analysis, as well as for fine-tuning and retraining the models. The purpose of this step is to evaluate whether the different methods can capture a reasonable degradation trend over time and to assess their stability and robustness. Specifically, this comparison examines whether the predicted results, when incorporating voyages with larger waves, remain consistent with those obtained using only BN-2 data in step 1. A stable and robust model should produce predictions that closely align with the reference results from step 1, even when more extensive datasets, including harsher sea conditions, are introduced.

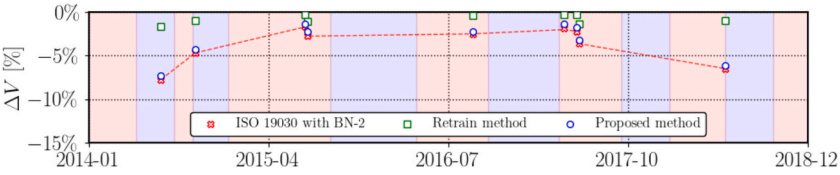

Fig. 14. Comparison of KPI (ΔV) for ship S1 calculated using the ISO 19030 standard (red scatter), the proposed freezing-based incremental learning method (blue scatter), and the retrain method (green scatter) with BN-2 filtering. The background colors represent intervals between cleaning events. (For interpretation of the references to colour in this figure legend, the reader is referred to the web version of this article.)

Table 3
KPI (ΔV) values for ship S1 obtained using ISO 19030 with BN-2 (reference), the proposed freezing-based incremental learning method, and the retrain method. It quantifies how closely each learning strategy reproduces the reference KPI derived from ISO 19030 with BN-2.

Voyage ID	ISO 19,030 with BN-2	Proposed method with BN-2	Retrain method with BN-2
1	7.73%	7.26%	1.62%
2	4.68%	4.23%	0.98%
3	1.69%	1.30%	0.30%
4	2.76%	2.22%	1.08%
5	2.49%	2.19%	0.42%
6	1.83%	1.38%	0.24%
7	2.20%	1.78%	0.28%
8	3.62%	3.16%	1.30%
9	6.47%	6.12%	0.98%

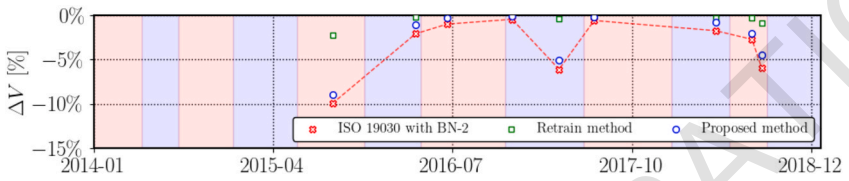

Fig. 15. Comparison of KPI (ΔV) for ship S2 calculated using the ISO 19030 standard (red scatter), the proposed freezing-based incremental learning method (blue scatter), and the retrain method (green scatter) with BN-2 filtering. The background colors represent intervals between cleaning events. (For interpretation of the references to colour in this figure legend, the reader is referred to the web version of this article.)

Table 4
KPI (ΔV) values for ship S2 obtained using ISO 19030 with BN-2 (reference), the proposed freezing-based incremental learning method, and the retrain method. It quantifies how closely each learning strategy reproduces the reference KPI derived from ISO 19030 with BN-2.

Voyage ID	ISO 19,030 with BN-2	Proposed method with BN-2	Retrain method with BN-2
1	9.93%	8.97%	2.13%
2	2.05%	1.09%	0.25%
3	0.98%	0.25%	0.05%
4	0.43%	0.06%	0.01%
5	6.09%	5.01%	0.48%
6	0.58%	0.14%	0.03%
7	1.78%	0.76%	0.36%
8	2.71%	2.03%	0.42%
9	5.90%	4.51%	1.04%

The results of the proposed method and the retrain method are presented in Figs. 16 and 17, respectively for ship S1, with the detailed KPI (ΔV) percentages listed in Table 5. For comparison, the ISO 19030 results obtained through default filtering are also included in the figures. The ΔV values derived from ISO 19030 with BN-2 filtering are plotted to serve as reference points, providing a benchmark for evaluating the accuracy of the different models.

As shown in Fig. 16 and Table 5, even after incorporating more data, including those associated with larger waves, the proposed method maintains a high degree of consistency with the ΔV values obtained from ISO 19030 with BN-2 filtering for the nine considered voyages. While the discrepancies are slightly larger compared to those in Table 3, where most differences were below 0.5%, the maximum discrepancy here remains within approximately 0.8%. This indicates that the proposed method effectively learns from new data during fine-tuning. Furthermore, a linear fit is applied to the predicted ΔV values across different intervals between cleaning events, as shown in Fig. 16. The proposed method successfully captures a reasonable degradation trend over time. The results clearly illustrate how the impact of biofouling gradually intensifies over time but is significantly alleviated following cleaning events.

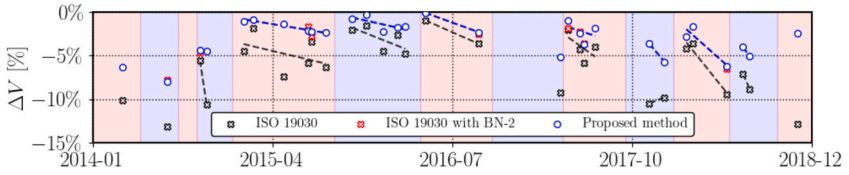

Fig. 16. Comparison of KPI (ΔV) for ship S1 calculated using the ISO 19030 standard (black scatter), and the proposed freezing-based incremental learning method (blue scatter) with default filtering. The background colors represent intervals between cleaning events. (For interpretation of the references to colour in this figure legend, the reader is referred to the web version of this article.)

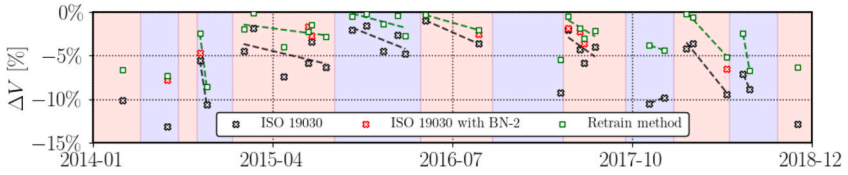

Fig. 17. Comparison of KPI (ΔV) for ship S1 calculated using the ISO 19030 standard (black scatter), and the retrain method (green scatter) with default filtering. The background colors represent intervals between cleaning events. (For interpretation of the references to colour in this figure legend, the reader is referred to the web version of this article.)

Table 5
KPI (ΔV) values for ship S1 obtained using ISO 19030 with BN-2 (reference), together with the proposed freezing-based incremental learning method and the retrain method evaluated under the default ISO 19030 filtering. It quantifies how closely each learning strategy under default filtering reproduces the reference KPI derived from ISO 19030 with BN-2.

Voyage ID	ISO 19,030 with BN-2	Proposed method	Retrain method
1	7.73%	8.02%	8.62%
2	4.68%	4.39%	2.51%
3	1.69%	2.11%	2.22%
4	2.76%	2.23%	1.62%
5	2.49%	2.28%	2.51%
6	1.83%	1.00%	0.44%
7	2.20%	2.41%	1.77%
8	3.62%	3.68%	3.12%
9	6.47%	6.25%	5.16%

Furthermore, the plot demonstrates that after dry docking, the biofouling-induced ΔV is substantially reduced, confirming the effectiveness of the intervention. In contrast, the trend derived from the ISO 19030 default filtering shows noticeable discrepancies compared to the proposed method's fitted trend. Notably, one interval even exhibits a reverse trend, indicating inconsistencies and potential inaccuracies when using the standard filtering approach.

For the retrain model, incorporating more data results in a noticeable reduction in the discrepancies between the predicted ΔV values and those obtained from ISO 19030 with BN-2 filtering. This behavior arises because the retrain method updates the entire ANN model using both new voyage data and the warm-up dataset, with all network parameters retrained simultaneously. When the amount of new voyage data is limited, as is the case after BN-2 filtering, the retrain model remains dominated by the warm-up data and lacks sufficient information to learn performance degradation patterns. As the filtering criterion is relaxed and more data becomes available, the retrain method can indeed improve its performance. As shown in Table 5, the maximum error is approximately 2.2%, which is still significantly higher than the errors achieved by the proposed method. Additionally, as illustrated in Fig. 17, the linear fit applied to the retrain model's results produces a relatively reasonable degradation trend, though it remains less accurate and consistent compared to the proposed method.

For the case study ship S2, the results are presented in Figs. 18 to 19 and Table 6. For the proposed method, after incorporating more data and larger wave conditions, the prediction errors for the nine voyages benchmarked against ISO 19030 with BN-2 filtering remain consistently low. The inclusion of larger waves even slightly improves the alignment of the predicted ΔV values with those obtained from ISO 19030 with BN-2 filtering. The maximum discrepancy remains within 1%, demonstrating the robustness of the proposed method. Moreover, the linear fit applied to the predicted ΔV values produce a reasonable trend, effectively detecting performance improvements following each cleaning event. The results also clearly show that, after dry docking, the biofouling-induced speed change for ship S2 is significantly alleviated.

The performance of the retrain method on ship S2 is notably less effective compared to its performance on ship S1 when applied to data filtered by the default ISO 19030 filtering. For the voyages benchmarked against ISO 19030 with BN-2 filtering, the prediction errors remain significantly high, with some discrepancies exceeding 7% (Voyage 1), as listed in Table 6. Other voyages (e.g., Voyages 6 and 7) exhibit physically unrealistic deviations, with predicted KPI values far exceeding those obtained from the ISO 19030 with BN-2 reference. This behavior indicates that, when exposed to larger volumes of new data, the retrain method may overly incorporate new information and forget previously learned representations, resulting in catastrophic forgetting. Such instability suggests that the reliability of the retrain model is worse than the proposed method. Furthermore, the linear fit applied to the retrain model's results, as shown in Fig. 19, reveals inconsistent trends across several intervals between cleaning events. In some cases, the model even indicates performance improvement where biofouling-induced degradation should be present, which is not consistent with the actual operational conditions.

6.3. Application of the proposed method to conditions without wind filtering

Based on the above comparison, the proposed incremental model has demonstrated superior capability in accurately capturing the biofouling impact on the two case study chemical tankers over a five-year data span. However, due to the ISO 19030 filtering criteria

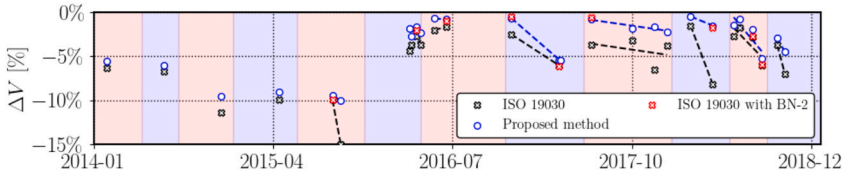

Fig. 18. Comparison of KPI (ΔV) for ship S2 calculated using the ISO 19030 standard (black scatter), and the proposed freezing-based incremental learning method (blue scatter) with default filtering. The background colors represent intervals between cleaning events. (For interpretation of the references to colour in this figure legend, the reader is referred to the web version of this article.)

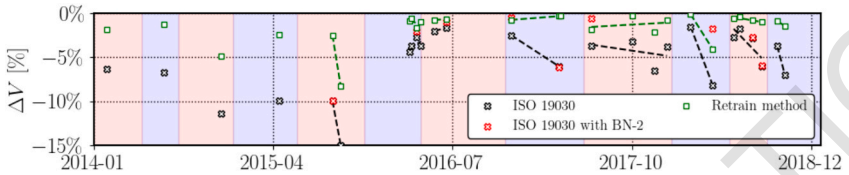

Fig. 19. Comparison of KPI (ΔV) for ship S2 calculated using the ISO 19030 standard (black scatter), and the retrain method (green scatter) with default filtering. The background colors represent intervals between cleaning events. (For interpretation of the references to colour in this figure legend, the reader is referred to the web version of this article.)

Table 6
KPI (ΔV) values for ship S2 obtained using ISO 19030 with BN-2 (reference), together with the proposed freezing-based incremental learning method and the retrain method evaluated under the default ISO 19030 filtering. It quantifies how closely each learning strategy under default filtering reproduces the reference KPI derived from ISO 19030 with BN-2.

Voyage ID	ISO 19,030 with BN-2	Proposed method	Retrain method
1	9.93%	9.45%	1.74%
2	2.05%	1.66%	1.72%
3	0.98%	0.51%	0.69%
4	0.43%	0.63%	0.52%
5	6.09%	5.42%	1.21%
6	0.58%	0.79%	1.98%
7	1.78%	1.50%	3.95%
8	2.71%	1.97%	0.63%
9	5.90%	5.28%	1.08%

for true wind speed, a substantial amount of data has been excluded from the analysis.

In this section, apart from the basic filtering of shallow water effects and sea water temperature as recommended by the ISO 19030 standard, no additional filtering of metocean data is applied. The primary objective is to ensure that a sufficient number of voyages are retained for analysis by avoiding overly strict filtering criteria. It allows for continuous monitoring of biofouling impacts without significant voyage data loss, which is crucial for capturing the gradual impact of biofouling over time. If the proposed method can successfully detect biofouling-induced performance degradation under more relaxed filtering conditions, it holds the potential for broader applicability in real-world ship operations.

For the case study ship S1, the distributions of significant wave height H_s and true wind speed without applying wind filtering are presented in Fig. 20. As shown, a substantial portion of the data exhibits true wind speeds ranging from 8 m/s to 10 m/s, which would have been excluded under the standard ISO 19030 filtering criteria. Additionally, the wave conditions cover a broader range,

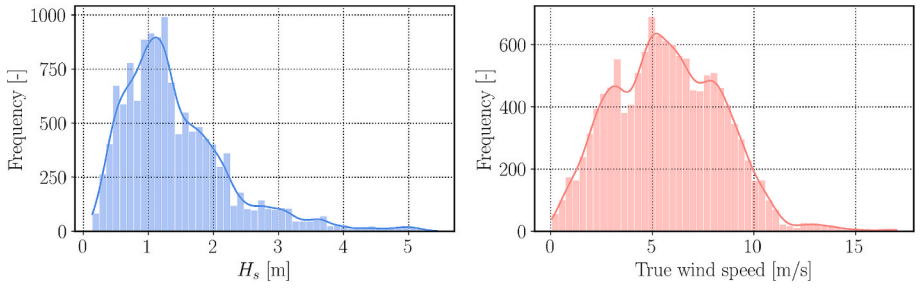

Fig. 20. Distributions of significant wave height H_s (left) and true wind speed (right) for ship S1 without wind filtering.

indicating a more comprehensive dataset that includes harsher sea states.

The ΔV values obtained by the proposed method are presented in Fig. 21. For reference, the ΔV results obtained from ISO 19030 with BN-2 filtering are also plotted to assess the accuracy of the proposed method. As shown in the figure, relaxing the stringent filtering criteria allows for a greater number of voyages and data points to be included in the analysis. Despite incorporating data associated with higher wind speeds and more severe wave conditions, the ΔV values predicted by the proposed method remain highly consistent with those obtained from ISO 19030 with BN-2 filtering for the benchmarked voyages. Although the discrepancies are slightly larger compared to the stricter filtering scenario, they remain within acceptable limits.

The KPI generated by the proposed method, along with the linear fits applied across different intervals between cleaning events, demonstrates a clearer detection of biofouling impact over time. The inclusion of more voyages improves the robustness of the identified degradation trend, while sudden changes due to cleaning events are effectively captured. Analysis of the linear fits reveals that approximately 1.5 years after dry docking, when the biofouling-induced speed reduction reaches around 4%, the shipowner initiates cleaning events for the hull or propeller. However, as the operation period extends further from dry docking, particularly during 2017 and 2018, cleaning events are often delayed until the speed reduction exceeds 5% or even approaches 8% before intervention occurs.

For ship S2, the distributions of significant wave height H_s and true wind speed without applying wind filtering are presented in Fig. 22. Similar to ship S1, the dataset now includes a broader range of wave conditions and true wind speeds, capturing more severe operational scenarios.

Before the middle of 2015, most voyages for ship S2 involved short-distance transport, resulting in limited data availability for analysis due to shallow water effect filtering. However, after mid-2015, the volume of usable data increased significantly compared to the stricter filtering approach. The ΔV values obtained by the proposed method for ship S2 are presented in Fig. 23. Despite incorporating data associated with larger waves for fine-tuning, the ΔV results produced by the proposed method remain relatively consistent with those obtained from ISO 19030 with BN-2 filtering. Moreover, the detected degradation trend appears more robust due to the inclusion of a broader range of operational conditions.

As shown in the figure, before dry docking, the shipowner initiated cleaning events when the biofouling-induced speed reduction exceeded approximately 10%. However, following the dry docking, maintenance actions were triggered more proactively, typically when the speed reduction reached around 3% to 4%. In some intervals, cleaning events were only performed when the reduction exceeded 5%.

The proposed incremental learning method offers significant gains for shipowners. By providing accurate and timely predictions of biofouling impact, shipowners can optimize the timing of hull and/or propeller cleaning events. This can result in more precise scheduling, either performing cleaning earlier to avoid excessive fuel consumption or delaying it to maximize operational efficiency without unnecessary maintenance. The method also offers the potential to avoid last-minute decisions, which can be costly due to limited dry docking slots and higher emergency costs. In the long term, adopting this approach can enhance energy efficiency and reduce overall maintenance costs.

7. Conclusion

This study proposes a physics-guided incremental learning method to assess the impact of biofouling on ship performance. Utilizing five years of full-scale measurement data from two sister chemical tankers, the proposed method integrates physics-informed neural networks, and freezing-based incremental learning to detect concept drift induced by biofouling. By applying warm-up data generated from PINNs trained on towing tank test results, a baseline model is established to characterize ideal ship performance under calm water conditions without biofouling or wave effects. The model is then incrementally fine-tuned using data collected over consecutive voyages. The effectiveness of the proposed approach is evaluated against the ISO 19030 standard and traditional retraining methods.

The key conclusions of this study can be summarized as follows:

- By employing a freezing technique, the proposed method effectively addresses the stability-plasticity dilemma, allowing the model to adapt to new data without catastrophic forgetting. The method successfully captures gradual performance degradation due to biofouling accumulation, as well as sudden improvements following cleaning events, which directly relate to variations in fuel consumption and GHG emissions.
- The proposed freezing-based incremental learning method demonstrates good capability in detecting biofouling-induced speed reduction, with discrepancies compared to ISO 19030 with BN-2 filtering generally within 1%. Even when larger wave conditions

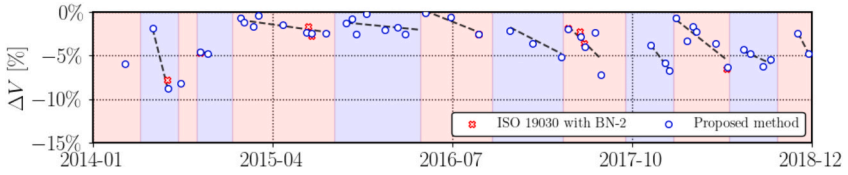

Fig. 21. KPI (ΔV) for ship S1 obtained by the proposed freezing-based incremental learning method (blue scatter) without true wind speed filtering. The background colors represent intervals between cleaning events. (For interpretation of the references to colour in this figure legend, the reader is referred to the web version of this article.)

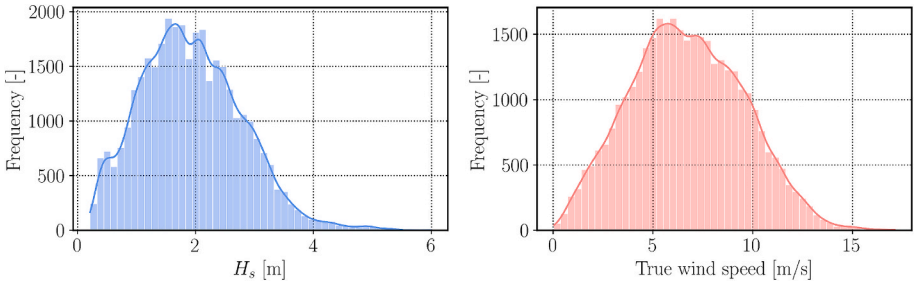

Fig. 22. Distributions of significant wave height H_s (left) and true wind speed (right) for ship S2 without wind filtering.

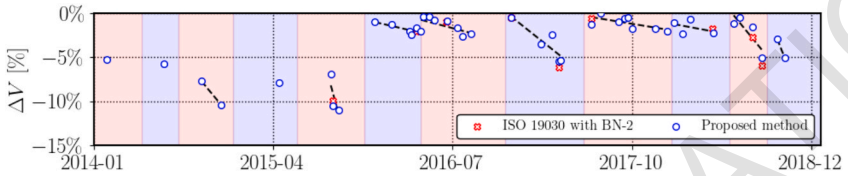

Fig. 23. KPI (ΔV) for ship S2 obtained by the proposed freezing-based incremental learning method (blue scatter) without true wind speed filtering. The background colors represent intervals between cleaning events. (For interpretation of the references to colour in this figure legend, the reader is referred to the web version of this article.)

with more data points are introduced for fine-tuning, the method retains robustness and accurately captures performance degradation trends, ensuring reliable energy efficiency monitoring.

- Unlike conventional filtering methods, the proposed framework shows robust performance even when metocean data filtering is relaxed. This adaptability highlights its potential for application in real-world operational scenarios where strict filtering criteria may not be feasible.
- Through continuous monitoring and incremental updates, the proposed framework provides shipowners with a comprehensive view of biofouling-induced performance degradation over time. The approach can detect degradation trends across multiple intervals between cleaning events, enabling predictive maintenance planning that improves energy efficiency, and minimizes the carbon footprint of vessel operations.

This work advances data-driven methodologies for ship performance assessment by integrating physics-based information with incremental learning techniques. By delivering accurate, timely predictions of biofouling impact, the proposed method enables shipowners to continuously monitor biofouling-induced performance degradation in percentage terms through post-voyage analysis, which is directly related to increased fuel consumption and emissions. This capability enables more informed, precise planning of cleaning schedules, either by conducting cleaning earlier to prevent excessive fuel consumption/GHG emission, or by postponing maintenance when acceptable performance can be maintained without unnecessary intervention. It prevents prolonged ship operation under degraded conditions. In addition, the proposed approach helps shipowners avoid last-minute maintenance decisions, which often result in higher costs due to limited dry-docking availability and emergency expenses. This contributes not only to cost-effective maintenance planning but also to achieving long-term decarbonization goals in line with international maritime regulations.

One key limitation of the present study is that both the involuntary speed reduction estimation and the warm-up data generation rely on a PINN model trained using towing tank experimental data. As a result, for ships lacking such experimental data, the applicability of the proposed framework may be constrained. In such cases, whether traditional semi-empirical methods for calm water speed estimation yield similar trends remains to be investigated. In addition, the proposed method has been validated using long-term full-scale data from two sister chemical tankers. Although the results demonstrate promising performance, further validation using larger datasets covering different ship types and operational profiles is necessary to fully assess the robustness and generalizability of the approach.

CRediT authorship contribution statement

Xiao Lang: Writing – review & editing, Writing – original draft, Visualization, Validation, Software, Methodology, Investigation, Formal analysis, Conceptualization. **Mingyang Zhang:** Writing – review & editing, Methodology, Investigation, Formal analysis, Conceptualization. **Wengang Mao:** Writing – review & editing, Supervision, Methodology, Investigation, Funding acquisition, Formal analysis, Conceptualization. **Jonas W. Ringsberg:** Writing – review & editing, Supervision, Investigation, Formal analysis, Conceptualization. **Nikolaos Tsoulakos:** Writing – review & editing, Formal analysis.

Declaration of Competing Interest

The authors declare that they have no known competing financial interests or personal relationships that could have appeared to influence the work reported in this paper.

Acknowledgments

This work was supported by the Trafikverket (Swedish Transport Administration) [grant No. TRV2023/98101]; the Vinnova (Swedish Governmental Agency for Innovation Systems) [grant No. 2021-02768]; and the Trafikverket/Lighthouse [grant No. FP14_2026]. The authors are also grateful to the ship owners for providing the full-scale measurement data.

Data availability

The authors do not have permission to share data.

References

Adland, R., Cariou, P., Jia, H.Y., Wolff, F.C., 2018. The energy efficiency effects of periodic ship hull cleaning. J. Clean. Prod. 178, 1–13. https://doi.org/10.1016/j.jclepro.2017.12.247.

Amante, C., Eakins, B.W., 2009. ETOPO1 1 Arc-Minute Global Relief Model: Procedures, Data Sources and Analysis. NOAA Technical Memorandum NESDIS NGDC-24. National Geophysical Data Center, NOAA.

Bialystocki, N., Konovessis, D., 2016. On the estimation of ship's fuel consumption and speed curve: a statistical approach. J. Ocean. Eng. Sci. 1 (2), 157–166. https://doi.org/10.1016/j.joes.2016.02.001.

Capezza, C., Coleman, S., Lepore, A., Palumbo, B., Vitiello, L., 2019. Ship fuel consumption monitoring and fault detection via partial least squares and control charts of navigation data. Transp. Res. Part D: Transp. Environ. 67, 375–387. https://doi.org/10.1016/j.trd.2018.11.009.

Carchen, A., Atlar, M., 2020. Four KPIs for the assessment of biofouling effect on ship performance. Ocean Eng. 217. https://doi.org/10.1016/j.oceaneng.2020.107971.

Carchen, A., Atlar, M., Turkmen, S., Pazouki, K., Murphy, A.J., 2019. Ship performance monitoring dedicated to biofouling analysis: Development on a small size research catamaran. Appl. Ocean Res. 89, 224–236. https://doi.org/10.1016/j.apor.2019.05.005.

Caric, H., Klobucar, G., Stambuk, A., 2016. Ecotoxicological risk assessment of antifouling emissions in a cruise ship port. J. Clean. Prod. 121, 159–168. https://doi.org/10.1016/j.jclepro.2014.08.072.

Copernicus Climate Change Service (C3S), 2019. ERA5: Fifth generation of ECMWF atmospheric reanalyses of the global climate. Copernicus Climate Data Store.

Coraddu, A., Lim, S., Oneto, L., Pazouki, K., Norman, R., Murphy, J., 2019a. A novelty detection approach to diagnosing hull and propeller fouling. Ocean Eng. 176, 65–73. https://doi.org/10.1016/j.oceaneng.2019.01.054.

Coraddu, A., Oneto, L., Baldi, F., Cipollini, F., Atlar, M., Savio, S., 2019b. Data-driven ship digital twin for estimating the speed loss caused by marine fouling. Ocean Eng. 186. https://doi.org/10.1016/j.oceaneng.2019.05.045.

Erol, E., Cansoy, C.E., Aybar, O.Ö., 2020. Assessment of the impact of fouling on vessel energy efficiency by analyzing ship automation data. Appl. Ocean Res. 105. https://doi.org/10.1016/j.apor.2020.102418.

Fan, A.L., Wang, Y.F., Hu, Z.H., Yang, L., Fan, X.L., Yang, Z.Y., 2025. Multi-dimensional performance verification of ship fuel consumption prediction model under dynamic operating conditions. Energy 332. https://doi.org/10.1016/j.energy.2025.137120.

Farkas, A., Degiuli, N., Martic, I., Ancic, I., 2020. Performance prediction method for fouled surfaces. Appl. Ocean Res. 99. https://doi.org/10.1016/j.apor.2020.102151.

Farkas, A., Degiuli, N., Martic, I., 2021. The impact of biofouling on the propeller performance. Ocean Eng 219. https://doi.org/10.1016/j.oceaneng.2020.108376.

Foteinos, M.I., Tzanos, E.I., Kyrtatos, N.P., 2017. Ship hull fouling estimation using shipboard measurements, models for resistance components, and shaft torque calculation using engine model. J. Ship Res. 61 (2), 64–74. https://doi.org/10.5957/Josr.61.2.160053.

French, R.M., 1999. Catastrophic forgetting in connectionist networks. Trends Cogn. Sci. 3 (4), 128–135. https://doi.org/10.1016/S1364-6613(99)01294-2.

García, S., Trueba, A., Boullosa-Falces, D., Islam, H., Soares, C.G., 2020. Predicting ship frictional resistance due to biofouling using Reynolds-averaged Navier–Stokes simulations. Appl. Ocean Res. 101. https://doi.org/10.1016/j.apor.2020.102203.

Gundermann, D., Dirksen, T., 2016. A statistical study of propulsion performance of ships and the effect of dry dockings, hull cleanings and propeller polishes on performance. Proc. 1st Hull Performance and Insight Conf. (HullPIC'16), Pavone, Italy.

Gupta, P., Rasheed, A., Steen, S., 2022. Ship performance monitoring using machine learning. Ocean Eng. 254. https://doi.org/10.1016/j.oceaneng.2022.111094.

Ikonomakis, A., Nielsen, U.D., Holst, K., Galeazzi, R., et al., 2021. How good is the STW sensor? an account from a larger shipping company. J. Mar. Sci. Eng. 9 (5), 465. https://doi.org/10.3390/jmse9050465.

IMO, 2012. Interim guidelines for the calculation of the coefficient for decrease in ship speed in a representative sea condition for trial use. International Maritime Organization, London.

IMO, 2014. Third IMO Greenhouse Gas Study 2014. International Maritime Organization, London.

IMO, 2020. Fourth IMO Greenhouse Gas Study 2020. International Maritime Organization, London.

IMO, 2022. Guidelines for the development of a ship energy efficiency management plan (SEEMP). International Maritime Organization, London.

IMO, 2023a. Revised IMO strategy on reduction of greenhouse gas emissions from ships. International Maritime Organization, London.

IMO, 2023b. Guidelines for the control and management of ships' biofouling to minimize the transfer of invasive aquatic species. International Maritime Organization, London.

ISO, 2015. Ships and marine technology - Guidelines for the assessment of speed and power performance by analysis of speed trial data 15016. International Organization for Standardization, Geneva.

ISO, 2016a. ISO 19030-1: Ships and marine technology – Measurement of changes in hull and propeller performance – Part 1: General principles. International Organization for Standardization, Geneva.

ISO, 2016b. ISO 19030-2: Ships and marine technology – Measurement of changes in hull and propeller performance – Part 2: Default method. International Organization for Standardization, Geneva.

ISO, 2016c. ISO 19030-3: Ships and marine technology – Measurement of changes in hull and propeller performance – Part 3: Alternative methods. International Organization for Standardization, Geneva.

I-Tech, 2020. Quantifying the scale of the barnacle fouling problem on the global shipping fleet. https://selektope.com/wp-content/uploads/2020/12/ITECH-WHITE-PAPER_June-2020-1.pdf [accessed 27 January 2025].

Jung, H., Ju, J., Jung, M., Kim, J., 2016. Less-forgetting learning in deep neural networks. arXiv:1607.00122. https://doi.org/10.48550/arXiv.1607.00122.

Karagiannidis, P., Themelis, N., 2021. Data-driven modelling of ship propulsion and the effect of data pre-processing on the prediction of ship fuel consumption and speed loss. Ocean Eng. 222. https://doi.org/10.1016/j.oceaneng.2021.108616.

Kjaer, L.L., Pigosso, D.C.A., McAloone, T.C., Birkved, M., 2018. Guidelines for evaluating the environmental performance of product/service-systems through life cycle assessment. J. Clean. Prod. 190, 666–678. https://doi.org/10.1016/j.jclepro.2018.04.108.
Koboevic, Z., Bebic, D., Kurtela, Z., 2019. New approach to monitoring hull condition of ships as objective for selecting optimal docking period. Ships Offshore Struct. 14 (1), 95–103. https://doi.org/10.1080/17445302.2018.1481631.
Lam, J.S.L., Lai, K.H., 2015. Developing environmental sustainability by ANP-QFD approach: the case of shipping operations. J. Clean. Prod. 105, 275–284. https://doi.org/10.1016/j.jclepro.2014.09.070.
Lang, X., Mao, W.G., 2020. A semi-empirical model for ship speed loss prediction at head sea and its validation by full-scale measurements. Ocean Eng. 209. https://doi.org/10.1016/j.oceaneng.2020.107494.
Lang, X., Wu, D., Mao, W.G., 2022. Comparison of supervised machine learning methods to predict ship propulsion power at sea. Ocean Eng. 245. https://doi.org/10.1016/j.oceaneng.2021.110387.
Lang, X., Wu, D., Mao, W.G., 2024. Physics-informed machine learning models for ship speed prediction. Expert Syst. Appl. 238. https://doi.org/10.1016/j.eswa.2023.121877.
Laurie, A., Anderlini, E., Dietz, J., Thomas, G., 2021. Machine learning for shaft power prediction and analysis of fouling-related performance deterioration. Ocean Eng. 234. https://doi.org/10.1016/j.oceaneng.2021.108886.
Li, Q., Lam, J.S.L., 2025. Biofuel consumption and emission prediction for harbour craft using machine learning methods. Transp. Res. Part D: Transp. Environ. 149, 105005. https://doi.org/10.1016/j.trd.2025.105005.
Logan, K.P., 2011. Using a ship's propeller for hull condition monitoring. Nav. Eng. J. 124.
Mittendorf, M., Nielsen, U.D., Bingham, H.B., 2023. Capturing the effect of biofouling on ships by incremental machine learning. Appl. Ocean Res. 138. https://doi.org/10.1016/j.apor.2023.103619.
Mittendorf, M., Nielsen, U.D., Gundermann, D., 2024. Monitoring hydrodynamic vessel performance by incremental machine learning using in-service data. Ship Technol. Res. https://doi.org/10.1080/09377255.2024.2362012.
Monty, J.P., Dogan, E., Hanson, R., Scardino, A.J., Ganapathisubramani, B., Hutchins, N., 2016. An assessment of the ship drag penalty arising from light calcareous tubeworm fouling. Biofouling 32 (4), 451–464. https://doi.org/10.1080/08927014.2016.1148140.
Munk, T., Kane, D., Yebra, D.M., 2009. The effects of corrosion and fouling on the performance of ocean-going vessels: a naval architectural perspective. In: Hellio, C., Yebra, D. (Eds.), Advances in Marine Antifouling Coatings and Technologies. Woodhead Publishing.
Owen, D., Demirel, Y.K., Oguz, E., Tezdogan, T., Incecik, A., 2018. Investigating the effect of biofouling on propeller characteristics using CFD. Ocean Eng. 159, 505–516. https://doi.org/10.1016/j.oceaneng.2018.01.087.
Parisi, G.I., Kemker, R., Part, J.L., Kanan, C., Wermter, S., 2019. Continual lifelong learning with neural networks: a review. Neural Networks 113, 54–71. https://doi.org/10.1016/j.neunet.2019.01.012.
Raissi, M., Perdikaris, P., Karniadakis, G.E., 2019. Physics-informed neural networks: a deep learning framework for solving forward and inverse problems involving nonlinear PDEs. J. Comput. Phys. 378, 686–707. https://doi.org/10.1016/j.jcp.2018.10.045.
Ramasesh, V., Dyer, E., Raghu, M., 2020. Anatomy of catastrophic forgetting: Hidden representations and task semantics. arXiv preprint arXiv:2007.07400. https://doi.org/10.48550/arXiv.2007.07400.
Schultz, M.P., 2007. Effects of coating roughness and biofouling on ship resistance and powering. Biofouling 23 (5), 331–341. https://doi.org/10.1080/08927010701461974.
Schultz, M.P., Bendick, J.A., Holm, E.R., Hertel, W.M., 2011. Economic impact of biofouling on a naval surface ship. Biofouling 27 (1), 87–98. https://doi.org/10.1080/08927014.2010.542809.
Shaw, H.J., Lin, C.K., 2021. Marine big data analysis of ships for the energy efficiency changes of the hull and maintenance evaluation based on the ISO 19030 standard. Ocean Eng. 232. https://doi.org/10.1016/j.oceaneng.2021.108953.
Song, S., Demirel, Y.K., Atlar, M., 2019. An investigation into the effect of biofouling on the ship hydrodynamic characteristics using CFD. Ocean Eng. 175, 122–137. https://doi.org/10.1016/j.oceaneng.2019.01.056.
Song, S., Demirel, Y.K., Atlar, M., 2020. Penalty of hull and propeller fouling on ship self-propulsion performance. Appl. Ocean Res. 94. https://doi.org/10.1016/j.apor.2019.102006.
Specht, D.F., 1991. A general regression neural network. IEEE Trans. Neural Netw. 2 (6), 568–576. https://doi.org/10.1109/72.97934.
Townsin, R.L., 2003. The ship hull fouling penalty. Biofouling 19, 9–15. https://doi.org/10.1080/0892701031000088535.
UNCTAD, 2023. World Investment Report 2023: Investing in Sustainable Energy for All. United Nations Conference on Trade and Development.
Uyanık, T., Karatuğ, Ç., Arslanoğlu, Y., 2020. Machine learning approach to ship fuel consumption: a case of container vessel. Transp. Res. Part D: Transp. Environ. 84, 102389. https://doi.org/10.1016/j.trd.2020.102389.
Uzun, D., Demirel, Y.K., Coraddu, A., Turan, O., 2019. Time-dependent biofouling growth model for predicting the effects of biofouling on ship resistance and powering. Ocean Eng. 191. https://doi.org/10.1016/j.oceaneng.2019.106432.
Valchev, I., Coraddu, A., Kalikatzarakis, M., Geertsma, R., Oneto, L., 2022. Numerical methods for monitoring and evaluating the biofouling state and effects on vessels' hull and propeller performance: a review. Ocean Eng. 251. https://doi.org/10.1016/j.oceaneng.2022.110883.
Yan, R., Wang, S., Psaraftis, H.N., 2021. Data analytics for fuel consumption management in maritime transportation: Status and perspectives. Transp. Res. Part E: Logist. Transp. Rev. 155, 102489. https://doi.org/10.1016/j.tre.2021.102489.
Yang, X., Wang, H., Zhang, R., Sun, S., Zhang, M., 2026. A deep learning method for spatiotemporal significant wave height estimation with ship attitude compensation. Ocean Eng. 352 (Part 1), 124517. https://doi.org/10.1016/j.oceaneng.2026.124517.
Zenisek, J., Holzinger, F., Affenzeller, M., 2019. Machine learning based concept drift detection for predictive maintenance. Comput. Ind. Eng. 137, 106031. https://doi.org/10.1016/j.cie.2019.106031.
Zhang, M., Tsoulakos, N., Kujala, P., Hirdaris, S., 2024. A deep learning method for the prediction of ship fuel consumption in real operational conditions. Eng. Appl. Artif. Intell. 130, 107425. https://doi.org/10.1016/j.engappai.2023.107425.